Modelling and optimisation of a natural gas liquefaction process

Joana Isabel Taborda Saldida Alves

Thesis to obtain the Master of Science Degree in

Chemical Engineering

Supervisor(s): Prof. Dr. Carla Isabel Costa Pinheiro
Dr. Klaas Maartÿn Nauta

Examination Committee

Chairperson: Prof. Dr. Sebastião Manuel Tavares Silva Alves
Supervisor: Prof. Dr. Carla Isabel Costa Pinheiro
Member of the Committee: Prof. Dr. Maria Cristina de Carvalho Silva Fernandes

November 2015

Everything is theoretically impossible, until it is done.

Robert A. Heinlein

Acknowledgments

First I would like to thank professors Carla Pinheiro and Costas Pantelides for the amazing opportunity to work at Process Systems Enterprise (PSE). I wish to thank also my supervisor Maarten Nauta for all the support, patience and the helpful advice given along the entire project. A special thanks to Mário that gave me such good ideas and showed me how to solve some problems. For all the precious help provided with the new challenge that C++ presented, a huge appreciation goes to Pierre Chevalier, my ”software-supervisor”.

To all my friends in PSE I thank for all the fun moments they provided me, and for making my London experience the best ever. Not forgetting my cool housemates, they caused me so many head aches but many more laughs, thank you for sharing your lives with me.

Finally, I would like to thank my family and my dear friends that have been with me through all the happy and motivated parts of my academical path, as well as the sad and frustrated ones that could not have been overcome without them.

Resumo

O objectivo deste projecto foi o desenvolvimento de um modelo matemático para um permutador de calor multi-corrente (MSHX) baseado na Análise do Pinch, nomeado modelo Pinch, e usar esse modelo em rápidas optimizações de processos criogénicos.

A liquefacção de gás natural (LNG) reduz o seu volume convertendo-o a uma forma mais fácil e segura de transportar. O LNG é produzido por refrigeração e uma unidade muito importante envolvida no ciclo de refrigeração é o MSHX. Para optimizar processos de LNG com objectivos económicos são necessários modelos de custo das unidades principais do processo.

O modelo Pinch determina balanços energéticos, curvas compostas, diferença mínima de temperatura entre correntes quentes e frias e factores de calor sobre diferença de temperatura que são introduzidos numa correlação para estimar o custo da unidade. O modelo funciona como esperado, o que foi comprovado com um software de integração energética.

O modelo Pinch foi integrado num ciclo de refrigerante misto de um andar, usado na liquefacção de gás natural, que foi optimizado com o objectivo de maximizar o lucro do processo. Os resultados e o tempo de optimização foram comparados com um caso de referência. Os resultados foram difíceis de comparar porque a inicialização das optimizações se mostrou muito divergente em termos de custo do permutador, devido a diferentes considerações assumidas nos modelos de MSHX distintos. A optimização aumentou o lucro em 41%. O tempo de optimização com a utilização do modelo Pinch em comparação com o caso de referência foi reduzido em 60%, o que infere um grande potencial no uso do modelo Pinch em optimizações rápidas de processos criogénicos. É de notar que os cálculos do Foreign Object que contém o algorítmo do Pinch representam apenas 0.5% do tempo total de optimização.

Keywords: Ponto de estrangulamento, Integração energética, Gás natural liquefeito, Permutador de calor multi-corrente, Criogénico

Abstract

The goal of this project was the development of a mathematical model for a multi-stream heat exchanger (MSHX) based on the Pinch Analysis, called Pinch model, and to use that model in fast optimisations of cryogenic processes.

Liquefaction of natural gas (LNG) reduces its volume making it easier and safer to transport. LNG is produced by refrigeration and a very important unit involved in the refrigeration cycles is the MSHX. In order to optimise LNG processes with economic objectives it is necessary to have costing models of the main units of the process.

The Pinch model determines heat balances, composite curves, minimum temperature approach between hot and cold streams and factors of duty over temperature difference that introduced in a correlation allow the estimation of the unit cost. It acted as expected which was validated with a heat integration software.

The Pinch model was integrated in a Single-stage Mixed Refrigerant cycle that was optimised with the objective of maximising the profit of the process. The optimisation results and time were compared with a reference case. The results were difficult to compare because the initialisation of the optimisations returned very divergent exchanger costs due to the different assumptions used in the distinct MSHX models. The optimisation increased the profit in 41%. The optimisation time reduction obtained with the Pinch model in comparison with the reference case was of 60% which infers a good potential in the use of the Pinch model in fast optimisations of cryogenic processes. It is important to notice that the calculations of the Foreign Object with the Pinch algorithm took only 0.5% of the total optimisation time.

Keywords: Pinch, Heat Integration, LNG, Multi-stream heat exchanger, Cryogenic

Contents

Acknowledgments v
Resumo vii
Abstract ix
List of Tables xiii
List of Figures xv
Nomenclature xvii
Glossary 1

1 Introduction 1
1.1 Motivation 2
1.2 Thesis Outline 3

2 Background 5
2.1 Natural Gas 5
2.1.1 Composition and Properties 5
2.1.2 Transport 6
2.1.3 Emission Levels 7
2.2 Natural Gas Market 8
2.2.1 Natural Gas Share 8
2.2.2 LNG Share 9
2.2.3 Liquefaction Technologies 9
2.2.4 Process Costs 10
2.3 LNG processing 10
2.3.1 Cascade cycles 11
2.3.2 Mixed refrigerant 13
2.3.3 Expansion turbine 13
2.3.4 Industrial processes 14
2.4 Multi-stream heat exchangers 19
2.5 MSHX models from literature 19

3 Pinch Analysis 21
3.1 Phase change 24

4 Materials and Methods 27

4.1 gPROMS software . . . 27

4.2 Foreign Objects . . . 27

4.2.1 Foreign Object interface . . . 28

4.2.2 Implementation of Foreign Objects . . . 29

4.2.3 C++ . . . 30

4.3 Multiflash package . . . 31

5 Multi-stream heat exchanger model 33

5.1 MSHX model . . . 34

5.2 Grid model . . . 36

5.3 Pinch FO . . . 37

5.3.1 PinchMS algorithm . . . 38

5.3.2 PinchUtilities method . . . 42

5.3.3 Algorithm validation . . . 45

5.3.4 Computational complexity . . . 45

5.3.5 Derivatives calculation . . . 46

6 Single-stage Mixed Refrigerant process optimisation 47

6.1 SMR process . . . 47

6.2 Reference case model . . . 48

6.2.1 Reference case heat exchanger model . . . 49

6.2.2 Process economics . . . 49

6.3 Problem formulation . . . 55

6.3.1 Initialisation . . . 58

6.4 Optimisation results . . . 59

6.5 Optimisation comparison with reference case . . . 60

6.5.1 Results . . . 60

6.5.2 Optimisation time . . . 62

7 Conclusions and future work 65

7.1 Conclusions . . . 65

7.2 Future work . . . 66

Bibliography 67

List of Tables

2.1 Natural gas typical composition [5]. 5
2.2 Natural gas properties [4]. 6
2.3 Air pollutants from fossil fuels [7]. 7

4.1 FO interface procedures and equivalents in C++ implementation. 30
4.2 Multiflash methods used in this work. 31

5.1 Inputs of the heat_exchanger_multistream model. 34
5.2 C values used in the correlation to estimate the MSHX cost [26]. 35
5.3 Inputs of the Grid model. 36
5.4 Inputs of the PinchMS method of the Pinch FO. 37
5.5 Outputs of the PinchMS method of the Pinch FO. 37
5.6 Inputs of the PinchUtilities method of the Pinch FO. 43
5.7 Outputs of the PinchUtilities method of the Pinch FO. 43

6.1 Notation of the variables in reference case model heat balance. 49
6.2 Variable costs constituents and respective contributions. 53
6.3 Fixed costs constituents and respective contributions. 54
6.4 CEPCI indexes. 55
6.5 Control variables, their bounds and initial guesses for optimisation. 57
6.6 Constrained variables and their limits in the optimisation problem. 57
6.7 Natural gas initial conditions. 58
6.8 Mixed refrigerant initial conditions. 58
6.9 Compressors initial conditions. 58
6.10 Coolers initial conditions. 58
6.11 Other process pressures in initial simulation. 59
6.12 Main cryogenic heat exchanger initial conditions. 59
6.13 Main results of the initial simulation. 59
6.14 Optimisation results of present work: decision variables. 60
6.15 Optimisation results of present work: constraints. 60
6.16 Initialisation results comparison. 61
6.17 Optimisation results comparison: controls. 61

6.18 Optimisation results comparison: MCHX cost and NPV. 61
6.19 Comparison of optimisation statistics. 62
6.20 Comparison of optimisation statistics with 49 iterations. 63
6.21 Foreign objects statistics in optimisation with Pinch model. 63

List of Figures

1.1 LNG supply chain [1]. 2

2.1 Natural gas reserves: top 5 countries [8]. 7
2.2 Global fuel shares of total primary energy supplies and electric generation [2]. 8
2.3 Historical and projected world energy demand by energy source (quadrillion Btu) [2]. . . . 8
2.4 Global Gas Trade, 2000-2013 (CAGR=compound annual growth rate) [9]. 9
2.5 Liquefaction capacity by type of technology, 2014-2020 [9]. 10
2.6 Average cost breakdown of liquefaction project by construction component [10]. 11
2.7 LNG production scheme [11]. 12
2.8 Refrigerant cycle in LNG production. 12
2.9 Cascade refrigeration scheme. 13
2.10 NG and refrigerant cooling curves. 13
2.11 General schematic of an expansion-turbine process. 14
2.12 Schematic of the C3-MR process. 15
2.13 Schematic of the AP-X^{TM} process. 15
2.14 Schematic of the ConocoPhillips Optimised Cascade®. 16
2.15 Schematic of the PRICO® process. 17
2.16 Schematic of the Statoil/Linde Mixed Fluid Cascade. 17
2.17 Schematic of the IFP/Axens Liquefin^{TM} process. 18
2.18 Schematic of the SDMR process. 19

3.1 Pinch technology scheme. 22
3.2 Composite curves and Pinch identification. 23
3.3 Composite curves divided in enthalpy intervals for the area calculation. 23
3.4 Typical variation of enthalpy with temperature of NG with phase change. 25

5.1 Schematics of the global MSHX model. 33
5.2 Topology representation of the heat_exchanger_multistream model. 34
5.3 PinchMS algorithm list of steps. 39
5.4 Assignment method used to complete new matrices or arrays. 40
5.5 Composite curves representation. 41

5.6 Demonstration of counter-current ΔT_{ln} determination with p representing points. The hot curve is flowing to the left while the cold curve is flowing to the right but both curves' arrays are ordered in ascending order. 41
5.7 Calculation steps of the PinchUtilities method. 44

6.1 SMR process used in optimisation. 48
6.2 Economic items involved in the life of a project. 50
6.3 Representation of the control variables used in optimisation of the SMR process. 57
6.4 Distribution of the fraction of each main equipment cost on total equipment cost for the SMR process. 59

Nomenclature

Greek symbols

δ	Small variation

Roman symbols

ΔH	Enthalpy variation
ΔH_{ac}	Accumulated enthalpy
ΔT_{ln}	Mean logarithmic temperature difference
ΔT_{min}	Minimum temperature approach between hot and cold streams
A	Heat transfer area
$allH$	Matrix with enthalpies corresponding to array allT for all streams (hot/cold)
$allT$	Array with the temperatures of all hot/cold streams
APC	Air Products and Chemicals Inc.
$areaH$	Array with the enthalpy points of both composite curves
$areaT$	Array with the temperatures of a composite curve
$auxH$	Matrix with the enthalpy points for all streams corresponding to the areaT arrays
Btu	British thermal unit
$BubblePoint$	Array containing the bubble point data of the streams
$C3-MR$	Propane mixed refrigerant
C_a	Cost expression
C_b	Cost expression
CF	Cash flow
CFD	Computational fluid dynamics
CIF	Construction inflation rate

$cond$	Binary array containing information on the stream condensability
Cp	Heat capacity
D	Annual depreciation
D	Internal diameter
DE	Delivered equipment
$DewPoint$	Array containing the dew point data of the streams
EIA	United States Energy Information Administration
F	Flowrate
f	Fugacity
F'	Correction factor for flow arrangement
F_M	Cost factor for material
F_T	Cost expression for type
FC	Fixed charges
FCI	Fixed-capital cost
FO	Foreign object
ft	Feet
GDP	Gross domestic product
GE	General expenses
GP	Annual gross profit
gPB	gPROMS ProcessBuilder
gpm	Gallon per minute
H	Specific enthalpy
h	Heat transfer coefficient
H'	Suction head
H_{vap}	Heat of vaporisation
HP	Compressor power
IFP	Institut Français du Pétrole (French Institute of Petroleum
$J-T$	Joule-Thomson

L	Height
LNG	Liquefied natural gas
M	Number of columns of the h and T grids
$MCHX$	Main cryogenic heat exchanger
MFC	Mixed fluid cascade
$MLTD$	Mean logarithmic temperature difference
MR	Mixed refrigerant
$MSHX$	Multi-stream heat exchanger
N	Number of streams
n	Input size (complexity)
nc	Number of components
NG	Natural gas
NGL	Natural gas liquids
NLP	Nonlinear programming
NP	Annual net profit
NPV	Net present value
OCF	Annual operating cash flow
OLC	Annual operating labour cost
or	Occupancy rate
P	Pressure
PC	Production costs
$PFHX$	Plate-fin heat exchanger
POC	Plant overhead costs
PSE	Process Systems Enterprise
Q	Heat transferred per unit of time
Q_v	Volumetric flowrate
Q_{CU}	Cold utility heat
Q_{HU}	Hot utility heat

r	Discount rate
S	Annual sales
$SDMR$	Shell dual mixed refrigerant
SMR	Single-stage mixed refrigerant
SQP	Sequential quadratic programming
$SumH$	Array with the sum of the enthalpies of all streams
$SWHX$	Spiral wound heat exchanger
Sz	Number of intervals of the composite curves
T	Temperature
t	Time of the cash flow
T'	Shifted temperature
TCI	Total capital investment
TPC	Annual total product cost
tr	Tax rate
U	Overall heat transfer coefficient
UtT	Array with the utility streams' temperatures
V_{in}	Inlet vapour fraction
V_{out}	Outlet vapour fraction
VC	Variable costs
vol	Binary array containing information on the stream volatility
W	Weight
w	Composition
WC	Working capital
y	Year of the process life
Z	Number of intervals to divide the streams' enthalpy and temperature sets

Subscripts

bub	Bubble point
$COLD$	Cold stream

$comp$	Component
dew	Dew point
HOT	Hot stream
i	Interval
j	Stream
p	Point

Superscripts

in	Inlet
l	Liquid phase
out	Outlet
v	Vapour phase

Chapter 1

Introduction

An environmentally friendly and efficient energy source, natural gas is the cleanest-burning conventional fuel, producing lower levels of greenhouse gas emissions than the heavier hydrocarbon fuels, like coal and oil. Historically, natural gas has also been one of the most economical energy sources, and gas plants can be built relatively quickly in around two years, unlike nuclear facilities, which can take much longer. Also, gas plants are flexible both in technical and economic terms, so they can react quickly to demand peaks, and are ideally twinned with intermittent renewable options such as wind power.

Natural gas fuels electric power generators, heats buildings and is used as a raw material in petrochemical industry to produce hydrogen, sulphur, carbon black, ethylene and ammonia. Natural gas is increasingly becoming a global commodity that is traded between regions. As such, international natural gas markets are undergoing a substantial change in market structure and organisation, as well as in supply and demand. Liquefying natural gas reduces its volume for easier and safer storage and transport which increases the importance of LNG role in the natural gas market as this is the physical form in which natural gas can be traded as a truly global commodity with transoceanic shipment from any region of supply to any region of demand. LNG also brought many large remote gas fields to the gas markets that are unreachable by pipeline [1].

LNG offers an opportunity to diversify energy supplies and with the decrease in its cost, it becomes more competitive in the gas markets. At a time of political instability, it can also be a more attractive option than international pipelines that cross multiple borders.

LNG supply chain is represented in Figure 1.1. At the exploration stage deposits of natural gas are detected (generally discovered during oil exploration operations) and during extraction (or production) the gas is drawn out to be available for treatment. Liquefaction converts the natural gas to its liquid form in which it can be transported by tanker at the shipping stage. Finally, there is the regasification step to restore the natural gas to its gas form in which it can be transmitted through pipelines for consumption by end customers.

The most important units in the liquefaction process are the heat exchangers because they rule the behaviour of the process and restrict the production and efficiency of the plant. The most used units in energy-intensive processes are the multi-stream heat exchangers due to their safe and cost-effective

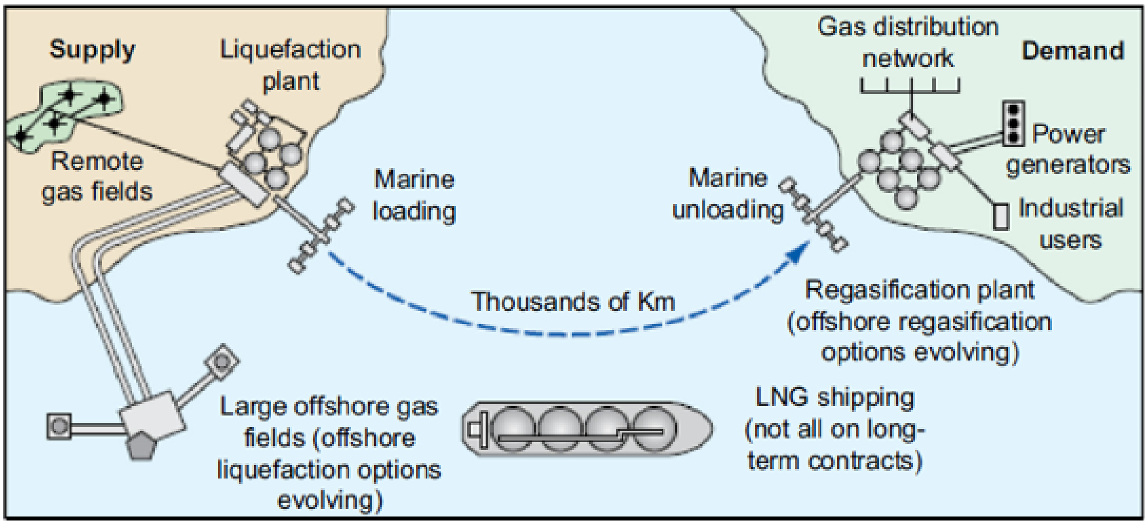
Supply
Liquefaction plant
Remote gas fields
Marine loading
Thousands of Km
Marine unloading
Gas distribution network
Demand
Power generators
Industrial users
Regasification plant (offshore regasification options evolving)
Large offshore gas fields (offshore liquefaction options evolving)
LNG shipping (not all on long-term contracts)

Figure 1.1: LNG supply chain [1].

designs and the need for higher effectiveness and efficiency.

In LNG plants heat exchangers represent 20 to 30% of the investment cost and their performance affects the sizing and designing of other equipment, namely compressors and their power drivers [2].

A model is an imitation of a real process and a mathematical model is a particular form of representation. Over the past decade there has been an increasing demand for suitable material in the area of mathematical modelling, because they represent a more convenient and economic tool to understand the factors that influence the performance of a system. Mathematical models are of great importance in chemical engineering because they can provide information about the variations in the measurable macroscopic properties of a physical system using output from microscopic equations which cannot usually be measured in a laboratory. Computer aided modelling, simulation and optimisation permit a better understanding of the chemical process behaviour, saves the time and money by providing the fewer configuration of the experimental work. In addition, computer simulation and optimisation can help to improve the performance and the quality of a process and represent a more flexible and cost effective approach in design and operation [3].

1.1 Motivation

With the prediction of increasing growth in LNG demand, the efforts to optimise the liquefaction technologies increase intensively. LNG projects are inherently capital-intensive, with the liquefaction process representing 30 to 40% of the capital cost. The liquefaction stage is then the best field to approach to make the largest cost savings because it has a greater influence in the project viability.

With the motivation in LNG growth and the importance of process modelling, the purpose of this work was to develop a mathematical model for multi-stream heat exchangers with cost prediction that could be integrated in cryogenic processes and result in fast optimisation runs. There is an existing model for this unit in ProcessBuilder libraries that determines the mass and heat balances but it lacks a tool for the cost calculation. This tool is essential to use the model in optimisation problems with economical objective functions, like the LNG flowsheet used as case study in the present work.

1.2 Thesis Outline

Chapter 2 presents a literature review on natural gas, the market shares and the liquefaction processes currently used in industry. Chapter 3 contains the description of the Pinch Analysis including calculation methods and assumptions. Chapter 4 describes the tools used in the development of the MSHX model including gPROMS platform, Foreign Objects (FO) and the property package Multiflash. The models developed in gPROMS and C++ are explicitly described in Chapter 5. Chapter 6 presents the formulation of the considered optimisation problem, including base case simulation, objective function, decision variables and process constraints, and the comparison of such optimisation problem with a reference case. Finally, Chapter 7 regards the conclusions of the project and suggestions for future work on the subject.

Chapter 2

Background

2.1 Natural Gas

Natural gas (NG) exists in nature under pressure in deep rock reservoirs, either associated with heavier hydrocarbons and water or by itself. It has been formed by the degradation of organic matter accumulated in the past millions of years [4].

2.1.1 Composition and Properties

The principal constituent of natural gas is methane. Water is almost always present as well as heavier hydrocarbons such as ethane, propane and butanes. In addition, it usually contains minor quantities of heavier hydrocarbons and varying amounts of gaseous nonhydrocarbons such as nitrogen, carbon dioxide, and hydrogen sulphide. A typical composition range is presented in table 2.1. This composition can vary widely depending on its source.

Table 2.1: Natural gas typical composition [5].

Compound	**Molar fraction**
Methane	0.75 - 0.99
Ethane	0.01 - 0.15
Propane	0.01 - 0.10
n-Butane	0.00 - 0.02
Isobutane	0.00 - 0.01
n-Pentane	0.00 - 0.01
Isopentane	0.00 - 0.01
Hexane	0.00 - 0.01
Heptane and higher hydrocarbons	0.00 - 0.001
Nitrogen	0.00 - 0.15
Carbon dioxide	0.00 - 0.30
Hydrogen sulphide	0.00 - 0.30
Helium	0.00 - 0.05

Natural gas is colourless, odourless, tasteless, shapeless, and lighter than air. Its main properties are in table 2.2.

Table 2.2: Natural gas properties [4].

Property	**Value**
Relative molar mass	17 - 20
Carbon content, weight %	73.3
Hydrogen content, weight %	23.9
Oxygen content, weight %	0.4
Hydrogen/carbon atomic ratio	3.0 - 4.0
Relative density, 15°C	0.72 - 0.81
Boiling point, °C	-162
Autoignition temperature, °C	540 - 560
Octane number	120 - 130
Methane number	69 - 99
Stoichiometric air/fuel ratio, weight	17.2
Vapour flammability limits, volume %	5 - 15
Flammability limits	0.7 - 2.1
Lower heating/calorific value, MJ/kg	38 - 50
Stoichiometric lower heating value, MJ/kg	2.75
Specific carbon dioxide formation, g/MJ	38 - 50

2.1.2 Transport

Transportation and storage of NG is difficult because of its low energy density at ambient temperature and pressure. There are several options for transporting NG from the fields to the market: pipelines, liquefied natural gas (LNG), compressed NG, gas to solids, gas to power and gas to liquids. The methods fully commercial and with mature technologies are pipelines and LNG. Pipelines are a convenient method of transport but are not flexible and the gas needs to be compressed to increase its energy content per unit of volume so that it can be economically transported. Besides, the storage of vapour requires huge underground caverns or large telescoping tanks.

Liquefaction serves to overcome the obstacles in pipeline transport, and permits transport over larger distances and more diverse application of the gas as an energy source. The principal reason for liquefying NG is the 1/600th volume reduction that occurs with the phase change. This method is very capital-intensive, however, it becomes economically feasible when the size of the reserves justify the capital investment of the LNG plant [6, 5].

Compressed NG is transported at high pressure, typically above 200 bars. Compressors and decompression equipment are less capital intensive and may be economical in smaller unit sizes than liquefaction/regasification plants. Natural gas trucks and carriers may transport natural gas directly to end-users, or to distribution points such as pipelines.

Gas to solids is a transportation method where NG is mixed with liquid water to form a crystalline substance (hydrate). This hydrate transport is still in the experimental stage but is believed to be a viable alternative to LNG and pipeline, having lower capital and operating costs.

Much of the transported gas destination is fuel for electricity generation. Electricity generation at or near the reservoir source and transportation by cable – gas to power - to the destination is possible but installing high-power lines is almost as expensive as pipelines and there is significant energy loss from the cables along the transmission line.

In gas to liquids processes the NG is converted to a liquid, such as syncrude methanol and ammonia, and is transported as such. These processes are complex and energy-intensive, and further developments continue to the present day [4].

2.1.3 Emission Levels

Natural gas is the cleanest of fossil fuels due to its low emission levels of pollutant gases. When combusted, its levels of sulphur dioxide are negligible and the levels of nitrous oxide and carbon dioxide are lower than other fossil fuels, see table 2.3. This fact reduces problems related to acid rain, ozone layer and greenhouse effect [6].

Table 2.3: Air pollutants from fossil fuels [7].

Pollutant (Billion Btus of energy)	Natural gas	Oil	Coal
Carbon dioxide	17 000	164 000	208 000
Carbon monoxide	40	33	208
Nitrogen oxides	92	448	457
Sulphur dioxide	1	1 122	2 591
Particulates	7	84	2 744
Mercury	0.0000	0.0007	0.016

Along with the environmental benefits, this fuel is also flexible and efficient for power generation having increased its contribution to the world energy economy. The reserves of conventional natural gas have grown by 36% over the past two decades and its production by 61%. In the period from 2010 to 2013 its reserves have grown 3% and production by 15%, see Figure 2.1 [8].

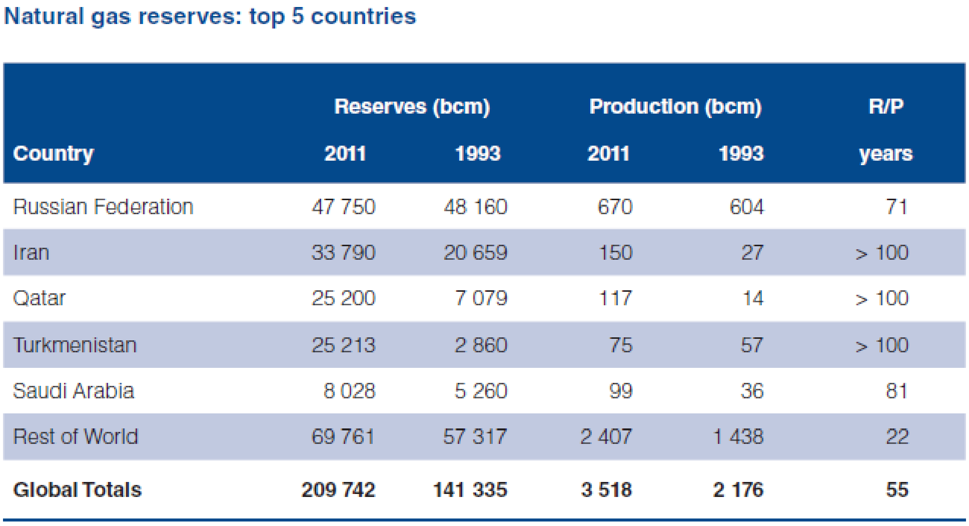

Natural gas reserves: top 5 countries

Country	Reserves (bcm) 2011	Reserves (bcm) 1993	Production (bcm) 2011	Production (bcm) 1993	R/P years
Russian Federation	47 750	48 160	670	604	71
Iran	33 790	20 659	150	27	> 100
Qatar	25 200	7 079	117	14	> 100
Turkmenistan	25 213	2 860	75	57	> 100
Saudi Arabia	8 028	5 260	99	36	81
Rest of World	69 761	57 317	2 407	1 438	22
Global Totals	**209 742**	**141 335**	**3 518**	**2 176**	**55**

Figure 2.1: Natural gas reserves: top 5 countries [8].

2.2 Natural Gas Market

2.2.1 Natural Gas Share

Natural gas accounts for 1/4 of global energy consumption. Over the last 20 years, the share of gas in the global energy mix has increased, while the share for oil has decreased, see Figure 2.2. These two trends are even stronger for the share of these fuels used for electric generation. This shift is driven by the generally lower price of natural gas compared to oil on an energy content (Btu) basis and the relatively lower costs of new natural gas electric generators. Further, the reduced emissions associated with natural gas use are increasingly important as many countries impose tighter emission standards.

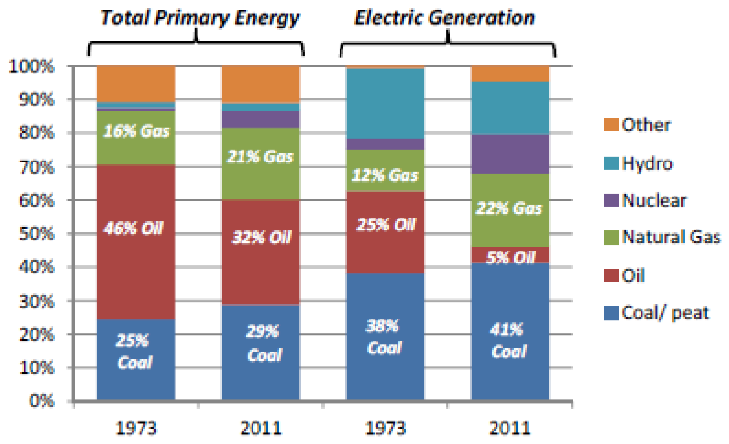

Figure 2.2: Global fuel shares of total primary energy supplies and electric generation [2].

In 2012, for the first time in many years, the growth in global gas demand outstripped that of coal. EIA projects natural gas demand will increase by about 64% from 116.8 Quads (1015 Btu) in 2010 to 191.3 Quads in 2040, as illustrated in Figure 2.3. These projections are based on assumptions for GDP growth and fossil fuel prices along with consideration of specific supply and demand issues [2].

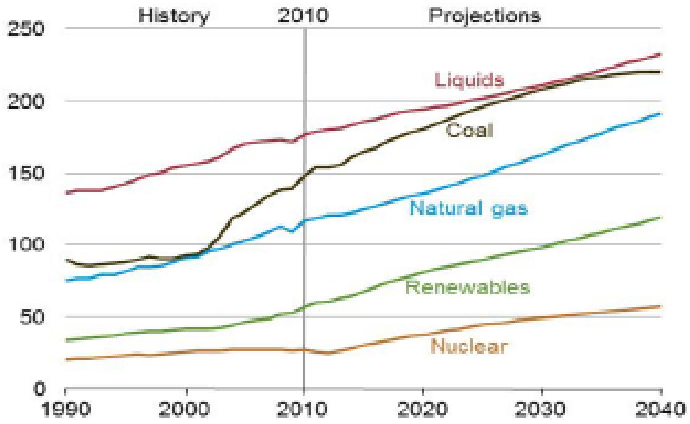

Figure 2.3: Historical and projected world energy demand by energy source (quadrillion Btu) [2].

This growth is supported by an increase in gas production potential and expansion of international trade based on a growing number of LNG facilities and high pressure pipelines and will continue for several decades. Natural gas is expected to continue its growth spurred by falling or stable prices, and thanks to the growing contribution of unconventional gas, such as shale gas. In addition to power generation, natural gas is expected to play an increasing role as a transport fuel.

2.2.2 LNG Share

The liquefied form of NG has been the fastest growing source of gas supply and now meets 10% of global demand. LNG is uniquely positioned to take a more commanding share of future gas consumption.

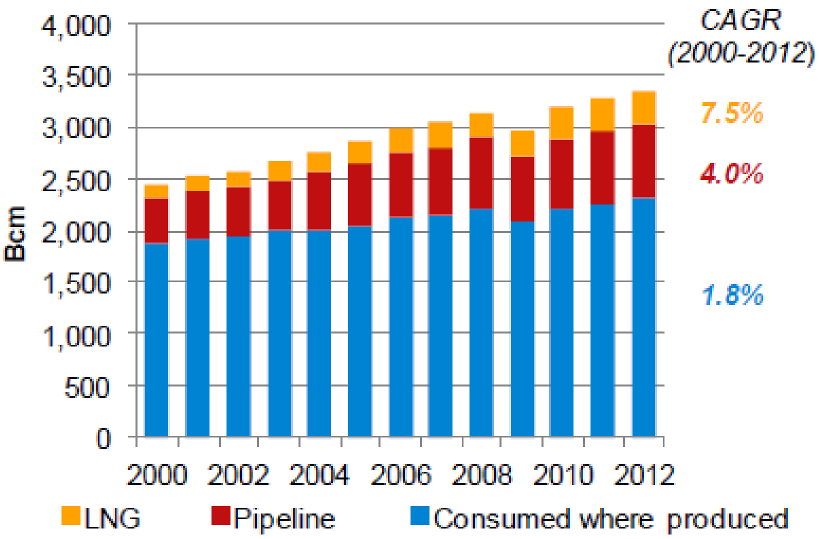

Figure 2.4: Global Gas Trade, 2000-2013 (CAGR=compound annual growth rate) [9].

Globally, the share of gas demand met by LNG has been rising quickly. In 1990, LNG made up just 4% of gas demand, but this has since grown to 10%. Other sources of gas supply remain more dominant (pipeline imports account for 21% and domestic production for 69%), but LNG is quickly catching up. LNG has been the fastest-growing source of supply, increasing by 7.5% per annum on average since 2000. This compares to slower growth of 4% per annum for pipeline imports and 1.8% per year for domestic production, as can be seen in figure 2.4 [9].

LNG is now considered safe and less polluting than other energy sources which originated its increasing demand. The demand is to be met by an increase in liquefaction plants and these are to be built with higher efficiency and in an environmentally responsible manner. This implies a constant development to enhance existing processes and lower its costs. LNG facilities are potentially very expensive but advances in technology have been reducing the costs associated with liquefaction and regasification [8].

2.2.3 Liquefaction Technologies

According to World LNG Report 2015 [10] about the liquefaction processes, in 2014 50% of existing liquefaction capacity utilised APC C3-MR , with another 30% split between AP-X and APC Split MR.

While the AP-X technology has exclusively been used in the Qatari mega-trains to date, several under construction projects have also selected the APC C3-MR or Split MR technology. Giving the large amount of capacity under construction, Air Products is expected to retain its leading position through 2020. However, its market share is set to fall to 73% as other new projects come online using competing technologies. The Optimised Cascade® technology will see particularly strong growth and its market share is set to rise from 13% to 21% by 2020, see figure 2.5.

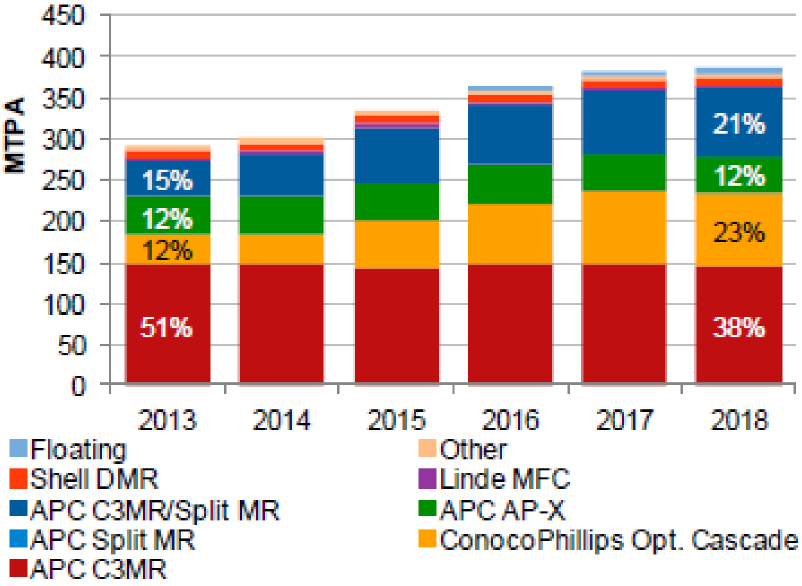

Figure 2.5: Liquefaction capacity by type of technology, 2014-2020 [9].

2.2.4 Process Costs

Cost has been the main challenge facing LNG projects worldwide. Liquefaction projects have faced considerable cost escalation since 2000 [10]. LNG plant costs vary widely and depend on location, capacity and liquefaction process. The number of storage tanks is also a large determining factor, as is access to skilled labour and the cost of moving through regulatory requirements and permitting. Large amounts of steel, cement and other bulk materials are required. Finally, investment in gas processing varies depending on the composition of the upstream resource. Gas treatment includes acid gas, natural gas liquids (NGL) and mercury removal, and dehydration. Figure 2.6 provides additional information on average liquefaction project costs by construction component [10].

The biggest slice corresponds to the liquefaction process and that is why the technologies used require continuous research in order to improve and optimise the processes and lower their cost.

2.3 LNG processing

The processes described in this section were taken from the literature [1, 6, 5]. Since it is extracted until it is liquefied, natural gas goes through a series of treatment processes such as sweetening, dehydration,

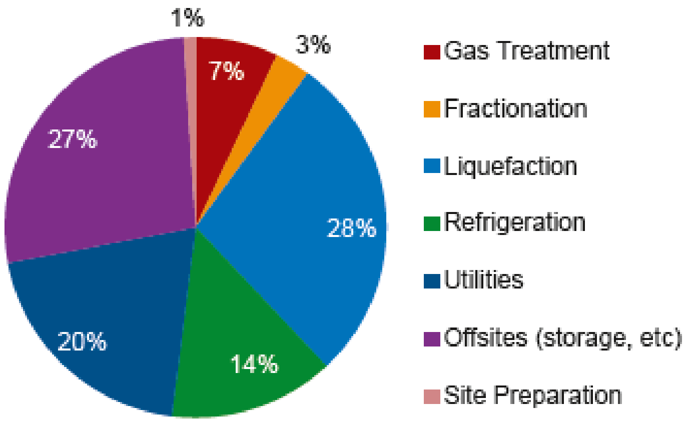

Figure 2.6: Average cost breakdown of liquefaction project by construction component [10].

mercury removal and liquids recovery as it is represented in figure 2.7.

The first block provides the physical separation of the gas from liquid hydrocarbons, condensed water and solids. This is performed in an inlet separator to prevent slugging of the transmission pipe. The next step is sweetening which provides the removal of acid gases such as carbon dioxide, hydrogen sulphide and other sulphur-containing species. In the presence of water these compounds form acids that are undesirable due to their corrosive properties. After sweetening there is the need of a dehydration process to meet sales gas specification and to control hydrate formation that causes choking/plugging of pipelines. The last step prior to liquefaction is hydrocarbon liquid recovery to meet specification and also because the liquid products have more value when sold as fuels than as sales gas components.

Liquefied natural gas is commercially produced by refrigeration instead of pressurisation because of the high critical pressure of methane. A number of processes have been commercialised for LNG production. Because the heat that must be removed from natural gas to cool it to approximately -160°C is eventually rejected to ambient air or water, rather elaborate systems have resulted.

A typical refrigerant cycle is presented in figure 2.8. In the main heat exchanger (green) the NG is liquefied while the refrigerant is vaporised. The refrigerant is then compressed, condensed and expanded in a Joule-Thompson valve where it is also further cooled to its final cooling duty that allows the liquefaction of the natural gas in the main heat exchanger closing the cycle.

Refrigerant cycles are used in all LNG processes, some with cascade to increase the efficiency and/or an expansion turbine instead of the Joule-Thomson (J-T) valve. The refrigerants used may be made of pure compounds or mixed refrigerants.

2.3.1 Cascade cycles

Cascade processes comply several refrigeration cycles with different refrigerants which make the process very efficient thermodynamically. A schematic of this method used in LNG production is represented in Figure 2.9.

LNG processes that use the cascade technology usually comprise 3 refrigerants: propane, ethylene

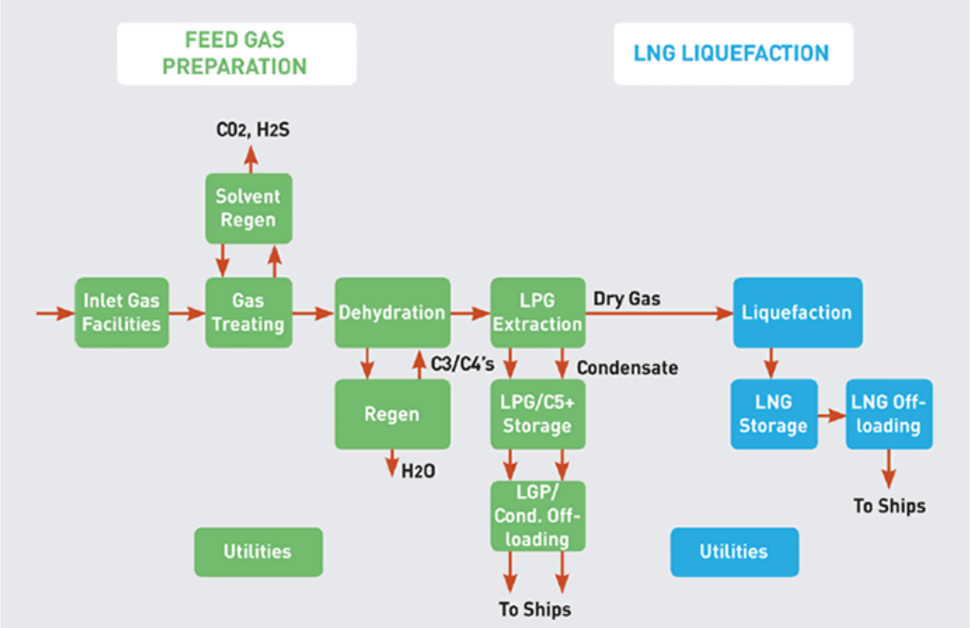
FEED GAS PREPARATION
LNG LIQUEFACTION
C02, H2S
Solvent Regen
Inlet Gas Facilities
Gas Treating
Dehydration
LPG Extraction
Dry Gas
Liquefaction
C3/C4's
Condensate
Regen
LPG/C5+ Storage
LNG Storage
LNG Off-loading
H2O
LGP/ Cond. Off-loading
To Ships
Utilities
Utilities
To Ships

Figure 2.7: LNG production scheme [11].

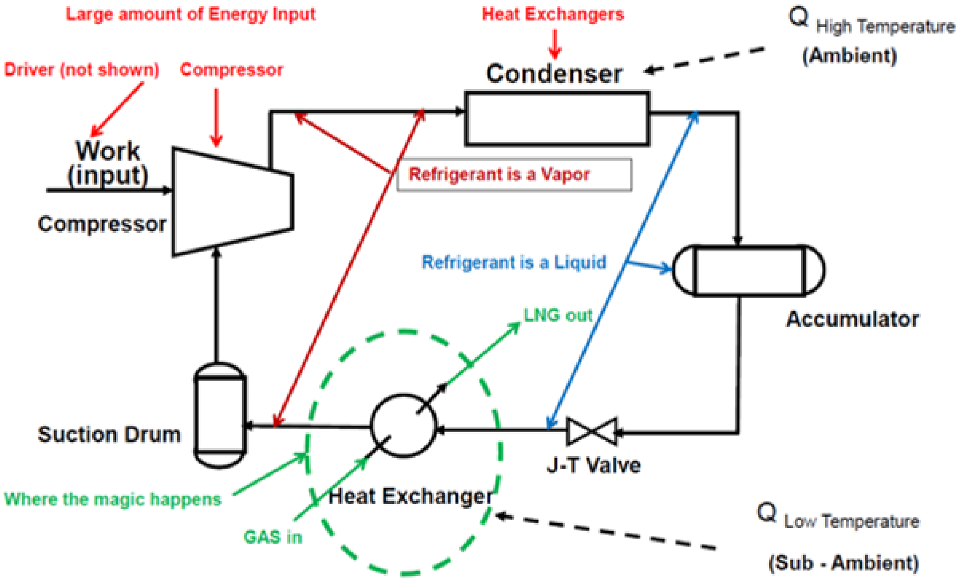
Large amount of Energy Input
Heat Exchangers
Q High Temperature
(Ambient)
Driver (not shown)
Compressor
Condenser
Work (input)
Refrigerant is a Vapor
Compressor
Refrigerant is a Liquid
Accumulator
LNG out
Suction Drum
J-T Valve
Where the magic happens
Heat Exchanger
GAS in
Q Low Temperature
(Sub - Ambient)

Figure 2.8: Refrigerant cycle in LNG production.

and methane. The process starts with a vapour that can be liquefied at ambient temperature by application of pressure only. The liquid formed by pressurisation is then expanded to a lower pressure, which results in a partial vaporisation and cooling of the remaining liquid. The cold liquid bath is then used to cool a second gas so that it may also be liquefied by the application of moderate pressure and then expanded to a lower pressure. The temperature reached in the expansion of the second liquid will be substantially lower than that achieved by the expansion of the first liquid. Each refrigerant is established as a separate close-loop refrigerator that supplies refrigeration at discrete temperature levels which makes this method very flexible in operation. In this fashion, heat is removed from the natural gas at successively lower temperatures. Heat is rejected to ambient air or water via the warmest refrigerant,

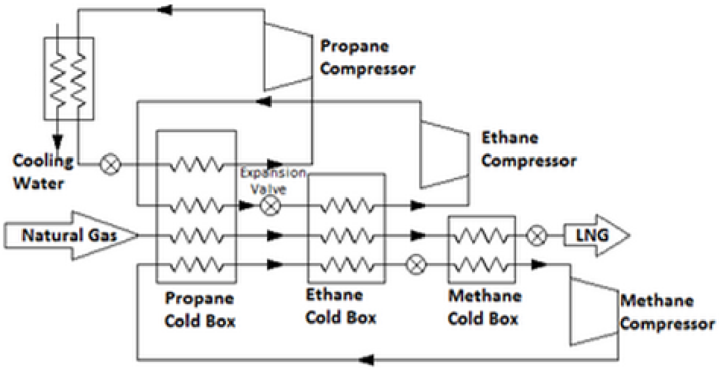
Propane Compressor
Ethane Compressor
Cooling Water
Expansion Valve
Natural Gas
LNG
Propane Cold Box
Ethane Cold Box
Methane Cold Box
Methane Compressor

Figure 2.9: Cascade refrigeration scheme.

generally propane.

2.3.2 Mixed refrigerant

The mixed refrigerant cycle involves the continuous cooling of a NG stream using a carefully selected blend of refrigerants, as pentane, butane, propane, ethane, methane and nitrogen, with the purpose of matching the cooling curve of natural gas (in orange) from ambient to cryogenic temperatures, so that energy usage and heat exchanger size can be optimised, figure 2.10.

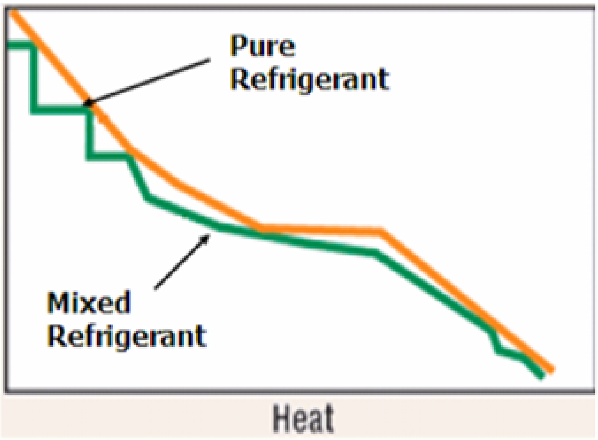

Figure 2.10: NG and refrigerant cooling curves.

This reduces the irreversibility of the process. The refrigerant mixture is compressed and then partially condensed in a water-cooled exchanger. Then it undergoes a series of pressure reductions and liquid-vapour separations to provide the necessary cooling duty to liquefy the NG.

2.3.3 Expansion turbine

The expansion-based gas liquefaction process uses turbo-expanders to produce the refrigerant. The turbo-expander cycle works by compressing and expanding a fluid to generate refrigeration. Expansion of high-pressure gas to the lower pressure in a reversible (or near) manner provides improvements over the Joule-Thomson expansion (valves). First, a large fraction of the work required to compress the gas can be recovered and used elsewhere in the cycle, which increases cycle efficiency. Second, the reversible process will result in a much larger cooling effect. The refrigerant, either nitrogen or methane, is a light volatile component that is an appropriate refrigerant for low temperature cooling. The expander cycle is less efficient when compared to the cascade and MR cycles, being more suitable for small LNG plants.

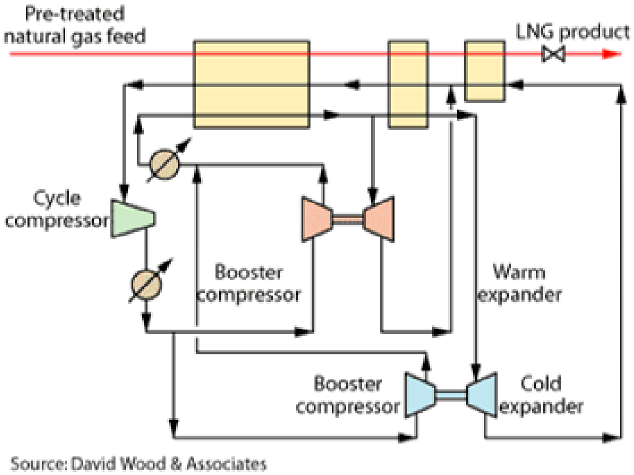

Source: David Wood & Associates

Figure 2.11: General schematic of an expansion-turbine process.

2.3.4 Industrial processes

The technologies currently used in the Industry to produce LNG are mainly the APC C3-MR and AP-X™; ConocoPhillips Optimised Cascade®; PRICO®; Statoil/Linde Mixed Fluid Cascade; IFP/Axens Liquefin™; and Shell Dual Mixed Refrigerant Process.

APC C3-MR

The Propane Precooled Mixed Refrigerant process was developed by Air Products & Chemicals Inc. and is the most widely used liquefaction process since the late 1970s, representing 75% of the LNG market.

Figure 2.12 shows the C3-MR process composed of a multistage propane precooling system and a MR system. The NG is initially cooled to approximately -35°C and then it is liquefied in the main cryogenic heat exchanger (MCHX). The MR is composed of nitrogen, methane, ethane and propane. The MR is partially condensed in the propane chiller and then both liquid and vapour streams are further cooled in the MCHX. After leaving the heat exchanger, the streams are expanded and cooled in J-T valves and re-enter the MCHX to provide the cooling for the hot streams. In this process, the MCHX is of the type spiral-wound, composed of many small-diameter tube bundles in a spiral.

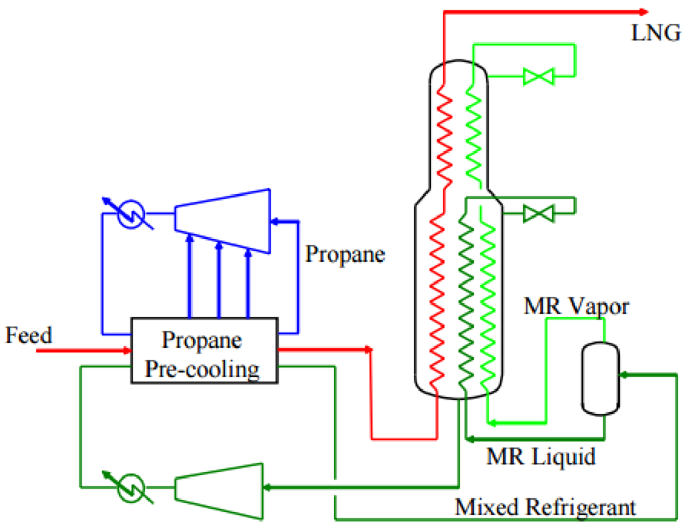
LNG
Propane
Feed
Propane
Pre-cooling
MR Vapor
MR Liquid
Mixed Refrigerant

Figure 2.12: Schematic of the C3-MR process.

AP-X^{TM}

AP-X^{TM} is an improvement to the C3-MR that makes greatly increased LNG capacity feasible. This process adds a third refrigerant cycle to provide the LNG subcooling duties outside the MCHX. The process is depicted in figure 2.13. Propane provides NG cooling to approximately -30°C, then NG is cooled and liquefied in the MCHX by the MR to -120°C and finally is subcooled in the nitrogen expander cycle.

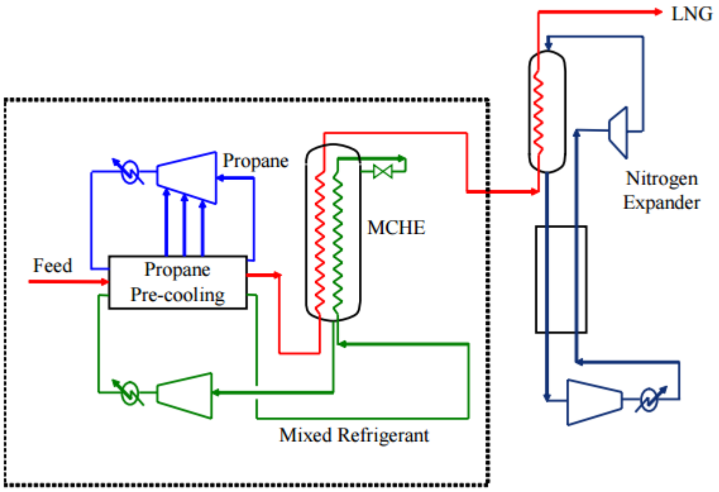
LNG
Propane
MCHE
Nitrogen
Expander
Feed
Propane
Pre-cooling
Mixed Refrigerant

Figure 2.13: Schematic of the AP-X^{TM} process.

ConocoPhillips Optimised Cascade®

Phillips Petroleum Company developed a cascade LNG process that uses propane and ethylene systems and a multistage methane refrigeration system to balance refrigeration loads. The process is represented in figure 2.14. NG is routed successively through each stage of propane and ethylene chillers. The compression heat in the propane cycle is removed by air or cooling water, while propane removes heat and condenses ethylene. Finally, NG is liquefied by methane that was cooled in the previous heat exchangers. The most commonly used heat exchangers in this process are brazed aluminium and core-in-kettle.

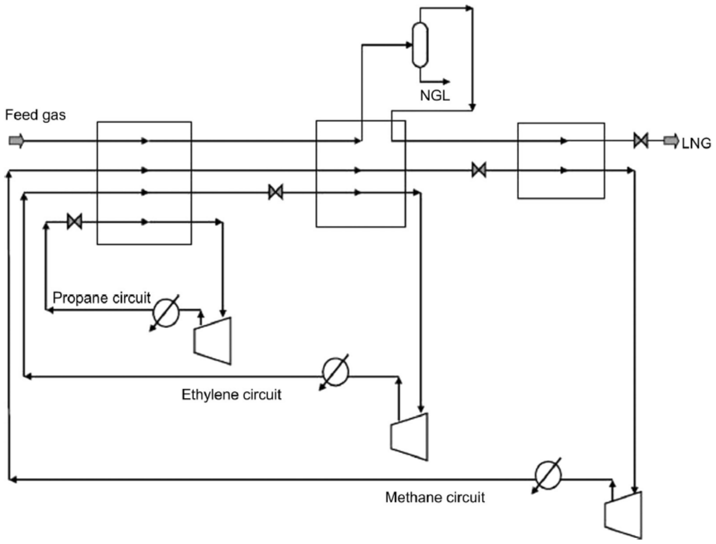

Figure 2.14: Schematic of the ConocoPhillips Optimised Cascade®.

PRICO®

The configuration of PRICO process by Black & Veatch Pritchard is shown is figure 2.15. It uses a single cycle of MR made up of nitrogen, methane, ethane, propane and isopentane. The NG stream is initially cooled to about -35°C and then the condensed heavy hydrocarbons are removed before the final cooling and liquefaction in the cold box. The MR is compressed and partially condensed before entering the cold box where it condenses totally and then it is flashed across an expansion valve that induces a temperature drop. The low pressure MR provides the chilling duty for the high pressure MR and NG streams. The cold box is a collection of highly efficient heat exchangers that help in the heat exchange process between the compressed refrigerant and the raw natural gas.

This process is considered as one of the simplest and most basic processes currently in operation in the industry. Though the simple setup limits the capacity per train, it reduces capital costs significantly. So this process is not as efficient as the multiple cycle process but it is suited and mainly used in smaller-scale and peak-shaving plants.

Statoil/Linde Mixed Fluid Cascade

The technology of Mixed Fluid Cascade (MFC) was developed by an alliance Statoil/Linde for the NG liquefaction in harsher environments. This process is a classic cascade with mixed components as refrigerants, improving the thermodynamic efficiency and operational flexibility when compared with the usual single component refrigerants, see figure 2.16.

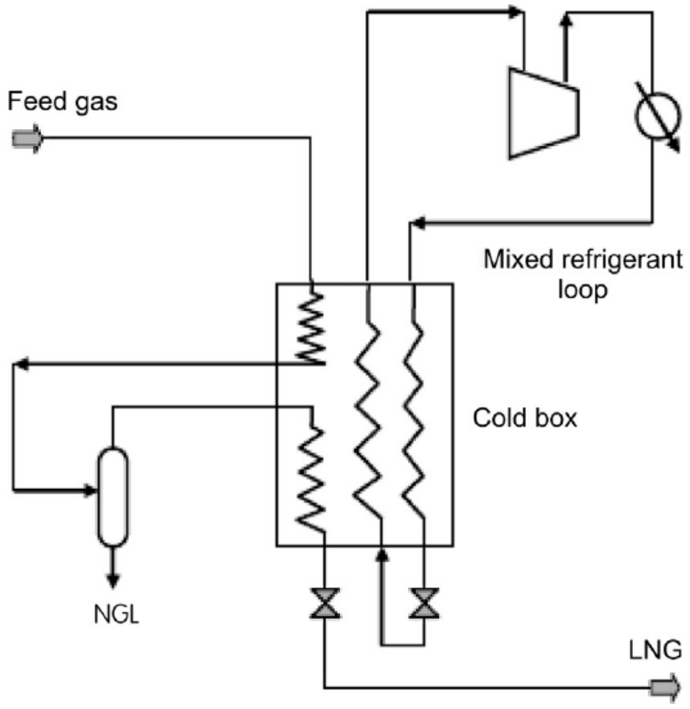
Feed gas
Mixed refrigerant loop
Cold box
NGL
LNG

Figure 2.15: Schematic of the PRICO® process.

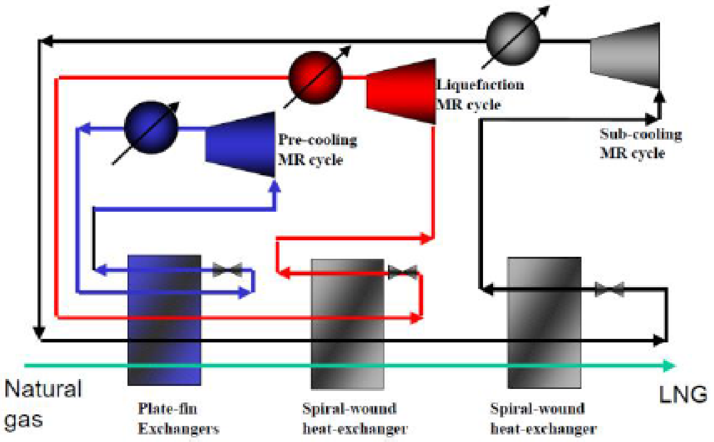
Liquefaction MR cycle
Pre-cooling MR cycle
Sub-cooling MR cycle
Natural gas
Plate-fin Exchangers
Spiral-wound heat-exchanger
Spiral-wound heat-exchanger
LNG

Figure 2.16: Schematic of the Statoil/Linde Mixed Fluid Cascade.

NG is precooled, liquefied and subcooled in three separate cycles. The refrigerants are made up of methane, ethane, propane and nitrogen. In the precooling cycle plate-fin heat exchangers are used, while in the other two cycles spiral-wound exchangers are preferred.

IFP/Axens Liquefin^{TM}

IFP and Axens proposed the Liquefin^{TM} process using a two-MR method as illustrated in figure 2.17. The NG stream is cooled between -50°C and -80°C with a MR (red) in the precooling section using plate-fin exchangers. After removal of heavy hydrocarbons, the NG passes in the cryogenic section being liquefied with a second MR (green). In the red cycle the MR is used at three different pressure levels to precool the NG. In the green cycle, the MR enters the top of the precooling section as a gas and leaves the cryogenic section totally condensed, and then it expands and re-enters the cryogenic section to provide the cooling duty for the hot streams.

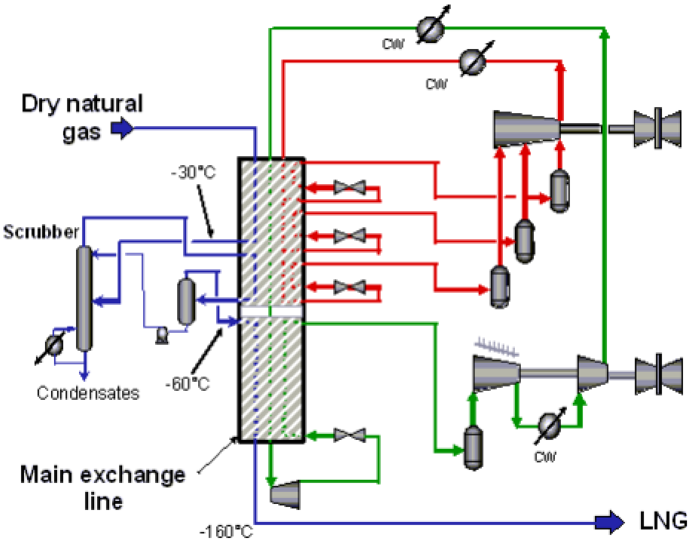

Figure 2.17: Schematic of the IFP/Axens Liquefin^{TM} process.

This process was developed with the aim of producing LNG cheaper than with any other process, at good conditions of reliability and safety, and more environment friendly.

Shell Dual Mixed Refrigerant process

Shell Dual Mixed Refrigerant process (SDMR) for NG liquefaction uses two MR cooling cycles, figure 2.18. One cycle is used to precool the NG to -50°C and the other to liquefy it. The precooling stage is similar to the propane precooling in C3-MR but with a MR of propane and ethane and using spiral-wound exchangers. The liquefaction MR is a mixture of nitrogen, methane, ethane and propane. The MR leaving the MCHX is compressed in a series of compressors with air intercooling. Further cooling and partial condensation is provided by the precooling MR cycle. The liquid and vapour are separated and cooled in the MCHX except from a small slip stream that is routed to the end flash exchanger.

Resuming the processes for the liquefaction of natural gas, in general the expander technology is favoured in small peak-shave plants, while the MR cycles are preferred for mid-scale facilities. For base-load plants, the used processes are propane precooled MR cycle, cascade or dual cycle due to their high efficiency.

All the processes above mentioned require the use of one or more multi-stream heat exchangers to provide the cooling and liquefaction of NG. This unit is one of high importance to regard in the process because it represents 20 to 30% of the investment cost of the LNG plant.

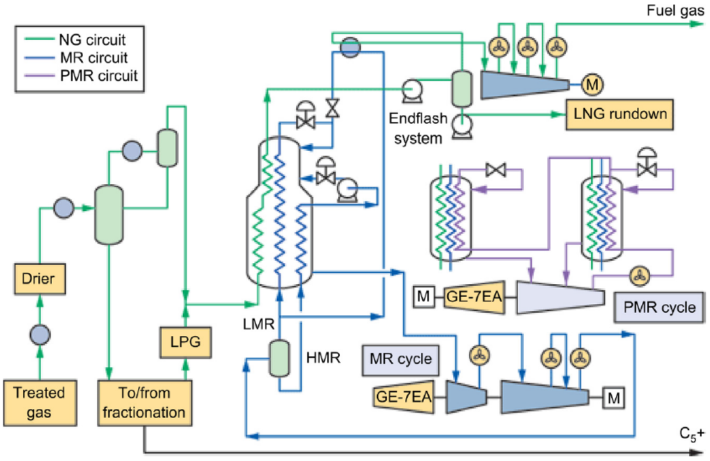

Figure 2.18: Schematic of the SDMR process.

2.4 Multi-stream heat exchangers

A multi-stream heat exchanger (MSHX) is a single process unit in which multiple hot and cold streams exchange heat simultaneously. MSHX are more popular in low temperature (cryogenic) applications, like LNG production, because these processes are dominated by requirements for very small temperature differences between streams exchanging heat due to the very high cost associated with compressor power to achieve the desired cryogenic temperatures. This leads to the necessity of exchangers that are highly compact, well insulated, and have a large number of flow passages for streams. The use of MSHX in cryogenic processes can result in significant savings in overall costs and space.

The main heat exchangers used in cryogenic applications are plate-fin heat exchangers (PFHX) and spiral (or coil) wound heat exchangers (SWHX). These types of exchangers have large internal surface areas consisting of a large number of heat exchanger cores or circuits. These designs can achieve a close temperature approach between the refrigerant and the natural gas in the liquefaction cycle [1].

2.5 MSHX models from literature

Literature research also provided information on existing models for MSHX developed in the past. 3 of these models were selected to introduce the study of MSHX modelling.

In 1990 Grossmann et al. [12] applied a superstructure model used in heat integration to a MSHX by fixing the utility consumption to zero reducing the model to an area targeting problem. The superstructure is a stage-wise representation where heat exchange can occur between each hot and cold stream. This model uses the assumption of vertical heat transfer in the area determination and enables simultaneous considerations for design factors without the limitations of a sequential analysis.

A model of a SWHX was published in 2007, also using the concept of superstructure [13]. The superstructure is a network of 2-stream heat exchangers including the possibility of heat transfer between all hot and cold streams by dividing the streams. This model regards phase change since this kind of exchanger is used in cryogenic processes. The change of enthalpy with temperature is assumed linear for single phase stage and for the double-phase stage equation 2.1 is applied where Q is the heat transferred per unit of time, H_{vap} is the heat of vaporisation, V represents the vapour fraction, F is the flowrate and Cp the heat capacity that uses a correlation to vary with F.

$$Q = H_{vap}(V_{in} - V_{out})F/Cp \tag{2.1}$$

In 2011 Kamath et al. [14] created an equation oriented model for a MSHX regarding phase change. Internally the model uses the Pinch concept to ensure minimum driving force criteria and the streams that are capable of phase change are split into substreams (one for each phase). This model is suitable for optimisation studies, particularly when the phases of the streams at the entry and exit of the unit are not known *a priori*.

These models generally cover the subject of modelling multi-stream exchangers and introduce the basis for the construction of the Pinch model in this project. This is a simpler model that follows the Pinch Analysis treating the process streams of a MSHX as the process streams of an entire process with zero utility consumption and regarding phase change.

Chapter 3

Pinch Analysis

Multi-stream heat exchangers are traditionally analysed using composite curves, a thermodynamic concept used in heat integration called Pinch analysis. Pinch analysis is a technique based on thermodynamic principles that offers a systematic approach to optimum energy integration in a process. The first law of Thermodynamics, also known as Law of Conservation of Energy, states that energy cannot be created or destroyed in a chemical reaction. The second law of Thermodynamics states that the entropy of an isolated system not in thermal equilibrium almost always increases. Using the first and second laws of Thermodynamics and the concept of temperature approach, this technology is used to design networks of heat exchangers through the identification of energy cost and network cost targets. The minimum temperature approach is defined by the minimum temperature difference, ΔT_{min}, that determines how closely the hot and cold composite curves can be without violating the Second Law [15]. The success of Pinch Technology has led to more inclusive ideas of process integration in which chemical processes are examined for both mass and energy efficiency. Even though process integration is a relatively new technology, its importance in process design is continuing to grow as processes become more complex. From the perspective of process modelling, MSHXs can be treated in the same way as heat exchangers' networks through the use of high level targeting models [14].

The Pinch technology technique begins by predicting the minimum requirements of external energy (utilities), network total heat transfer area, and number of units (exchangers) for a given process at the Pinch point that is the most constrained point of the network. Then there is the construction of the network that satisfies the energy targets, and finally the optimisation of the network so that the total cost is minimised. The main steps of the Pinch analysis are represented in figure 3.1.

The identification of the streams as hot or cold is based on the inlet and outlet temperatures or enthalpies. The input data required to perform the Pinch Analysis for heat exchangers networks comprises inlet and outlet temperatures, flowrates, heat capacities and heat transfer coefficients for all the streams involved in the process. The selection of the initial ΔT_{min} can be made using the typical industrial values for a specific case. The above mentioned data is required to build the composite curves. In composite curves the hot streams flow in one direction, while the cold streams flow in the opposite direction. All hot streams are merged into one pseudo-stream, the hot composite curve, while all cold streams are

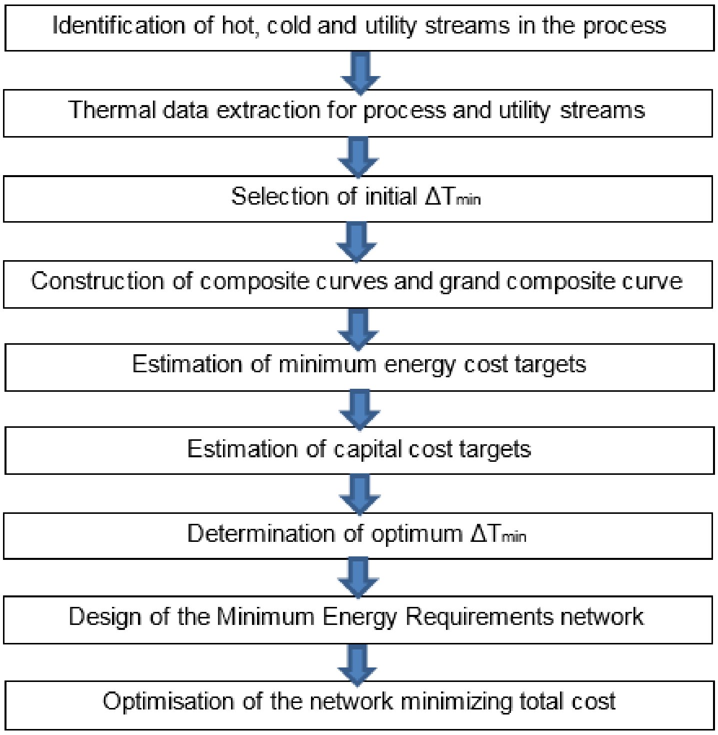
Identification of hot, cold and utility streams in the process
Thermal data extraction for process and utility streams
Selection of initial ΔTmin
Construction of composite curves and grand composite curve
Estimation of minimum energy cost targets
Estimation of capital cost targets
Determination of optimum ΔTmin
Design of the Minimum Energy Requirements network
Optimisation of the network minimizing total cost

Figure 3.1: Pinch technology scheme.

merged into the cold composite curve. Globally, the curves represent the cumulative heat content of all hot and cold streams (separately).

The composite curves allow the determination of the minimum utility requirements as well as the identification of the Pinch point but not in a very accurate way as it is based on a graphical construction. A numerical approach called Problem Table Algorithm, or Heat Cascade, was developed by Linnhoff & Flower (1978) as means of determining the utility needs of a process and the location of the pinch point in a more accurate manner. The base idea of the method is to verify, for each interval of temperatures, the energy amount available between the process streams involved in the interval and transfer the excess of energy of a thermic level to the level below.

The composite curves can be used to evaluate the overall trade-off between energy and capital costs. An increase in ΔT_{min} causes the energy costs to increase, with the increase in utility requirements, but also provides larger driving forces for heat transfer, so smaller area, and accompanying reduced capital costs. The Pinch point is where the design of the network is most constrained, where ΔT_{min} happens.

Once identified the Pinch, the process is then considered as two separate systems: one above and one below the Pinch, figure 3.2. The system above the pinch requires a heat input and is therefore a net heat sink. Below the pinch, the system rejects heat and so it is a net heat source. The understanding of the Pinch gives three rules that must be obeyed in order to achieve the minimum energy targets for a process:

- Heat must not be transferred across the Pinch;
- There must be no external cooling above the Pinch;

- There must be no external heating below the pinch.

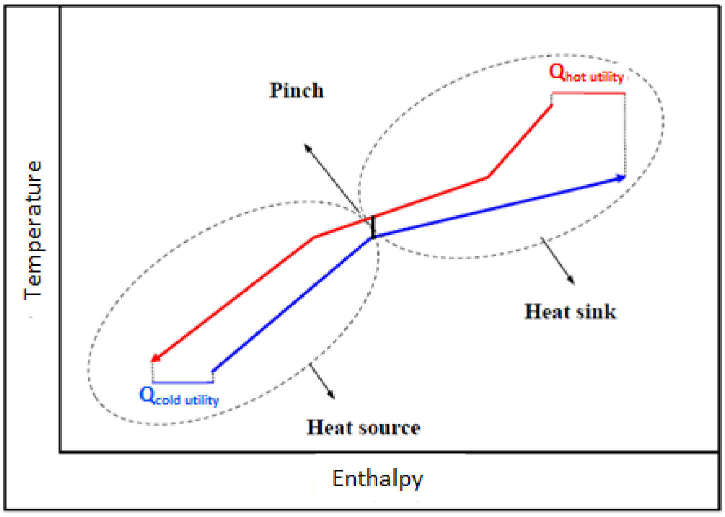

Figure 3.2: Composite curves and Pinch identification.

Violating any of these rules will lead to cross-pinch heat transfer resulting in an increase in the energy requirement beyond the target [16].

The grand composite curve allows for the choice of the best utility levels for the process, indicating the difference between the heat available from the process hot streams and the heat required by the process cold streams, relative to the Pinch, at a given shifted temperature.

The estimation of the capital costs involves the calculation of the equipment cost. This calculation is usually made with a correlation that depends on the type of exchanger, the material used in its construction and the heat transfer area. The composite curves are also used to determine the minimum heat transfer area required to achieve the energy targets. For this, the curves are further divided in enthalpy intervals such as in each interval neither curve changes slope, as shown in figure 3.3.

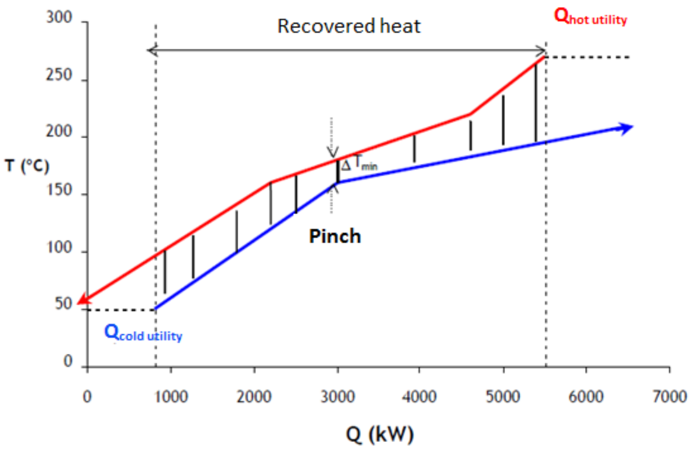

Figure 3.3: Composite curves divided in enthalpy intervals for the area calculation.

This area target is based on the assumption that “vertical” heat exchange will be adopted between the hot and the cold composite curves across the whole enthalpy range. The area is calculated for each enthalpy interval and the total network area is considered to be the sum of all the areas, as explicit in equation 3.1, where *i* and *j* are intervals and streams respectively.

$$A = \sum_i \left(\frac{1}{\Delta T_{ln,i}} \sum_j \frac{Q_{ji}}{h_{ji}} \right) \tag{3.1}$$

A is the total heat transfer area of the network, ΔT_{ln} is the mean logarithmic temperature difference (MLTD), Q is the heat transferred for each stream in each interval and h is the stream heat transfer coefficient or film coefficient. MLTD is calculated assuming counter-current heat exchange, equation 3.2. This equation can be used to target heat transfer area, within 10% of the actual minimum of the heat exchanger network on the basis of a vertical exchange shown in figure 3.3, if heat transfer coefficients do not present large variations between streams [17].

$$\Delta T_{ln} = \frac{(T^{in}_{HOT} - T^{out}_{COLD}) - (T^{out}_{HOT} - T^{in}_{COLD})}{ln \left[\frac{(T^{in}_{HOT} - T^{out}_{COLD})}{(T^{out}_{HOT} - T^{in}_{COLD})} \right]} \tag{3.2}$$

Low values of ΔT_{min} can result in large and costly heat exchangers but the utilities required increase as the heat exchanger area decreases. While there are cost savings involved with decreasing the physical area of the exchanger, there are high energy costs associated with an increase in utilities. With energy and capital costs determined, it is possible to find the optimum ΔT_{min} that minimises the total cost and then repeat the previous calculations to determine new targets.

The next step is to build the network by dividing it by the Pinch and matching the streams to define the location of the exchangers, respecting the energy target. Finally this network is optimised in order to minimise the total costs, by allowing an energy penalty while reducing the number of exchangers. These last two steps are not relevant for the work done during this thesis as they refer to the design of the network itself and here it is developed a simple model for a single MSHX.

In summary, the benefit of using Pinch analysis in this project is related to the fact that composite curves not only provide information about energy targets but also help predicting heat transfer area of the network or, in this case, the MSHX. Moreover this method is also capable of ensuring the minimum driving force criteria.

3.1 Phase change

Heat integration technology relies on an assumption of constant heat capacity flowrate. Typically the heat capacity does not vary significantly with temperature in the subcooled and superheated regions, which are in a single phase, though when phase change occurs this assumption does not hold. A cryogenic process like LNG mainly utilises the vaporisation of mixed refrigerants to cool, liquefy and sub-cool natural gas, figure 3.4. This is especially important for multi-component streams where the phase change occurs over a large temperature range.

To overcome this issue, a piecewise linearisation can be applied to the variation of enthalpy with temperature dividing this relation in small intervals which temperature-enthalpy pairs (T, H) contain the

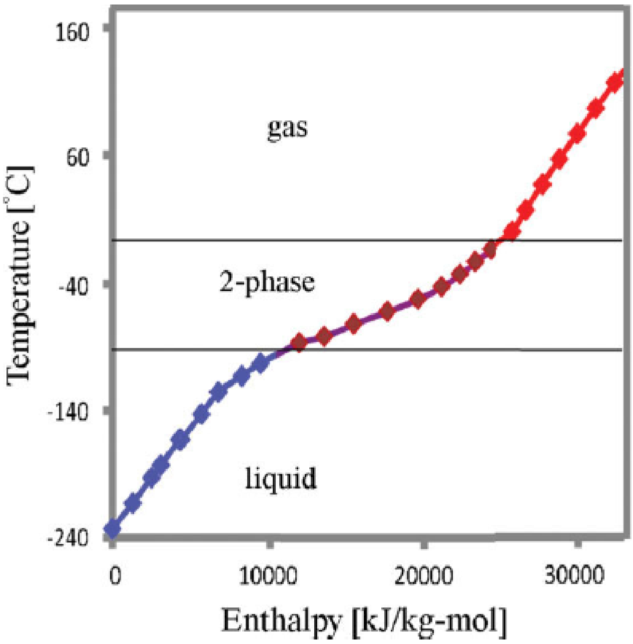

Figure 3.4: Typical variation of enthalpy with temperature of NG with phase change.

dew and bubble points to track the phase change. The variation of enthalpy with temperature is then assumed to be linear inside each interval [18].

As one of the objectives of this work is to build a model for a MSHX that is mainly used for cryogenic applications where change of phase occurs, this approach is used to increase the accuracy of the model regarding the physical properties of the streams.

Chapter 4

Materials and Methods

4.1 gPROMS software

The software used in the construction of the model was gPROMS®, a platform for high-fidelity predictive modelling for the process industries developed by Process Systems Enterprise (PSE). It is the foundation on which all of PSE's gPROMS family modelling and optimisation products are built. The main applications of gPROMS family products are in model-based engineering activities for process and equipment development and design, and optimisation of process operations.

gPROMS ProcessBuilder is an Advanced Process Simulation tool for model-based support of key design and operating decisions. ProcessBuilder also provides all the power of the gPROMS platform in an easy-to-use flowsheeting environment that contains industry-leading steady-state and dynamic process models. ProcessBuilder supports the complete workflow from basic design calculations based on steady-state mass and energy balances, to steady-state rating calculations, all the way to dynamic modelling of processes and their control systems [19].

Another feature of gPROMS ProcessBuilder is the optimisation tool which can be used to optimise steady-state and dynamic behaviour of continuous flowsheet, considering design and operation variables. An objective function is minimised or maximized by manipulation of a group of control variables. The optimisation problem may be subject to inequality and equality constraints to respect the process operational limits. The optimisation solver used by gPROMS was the NLPSQP solver that employs a sequential quadratic programming (SQP) method for the solution of a nonlinear programming (NLP) problem, as the optimisation problem in the present work is non-linear [20].

4.2 Foreign Objects

gPROMS also allows the use of external software components, called Foreign Objects (FO), that provide certain computational services to gPROMS models. These include physical property packages, external unit operation modules, or even complete computational fluid dynamics (CFD) software packages [21]. The present work required the use of this feature, the Pinch analysis algorithm was adapted to a MSHX and developed as a FO. This section presents the description of the interface and implementation of a FO in gPROMS platform.

The main reasons to use an external software package to express relationships between some of the variables in a gPROMS model are:

- The relationship cannot be expressed conveniently in closed algebraic form without the introduction of many intermediate quantities;
- The relationship involves many data parameters that would have to be extracted first and then inserted manually in the gPROMS model;
- The software that carries out the required calculation already exists and is tested so it would be wasteful to have to reproduce its functionality in gPROMS.

The FO is an independent software and the only way one can access any information relating to it is by making use of a well-defined interface that it provides to the outside world.

Each Foreign Object provides a set of methods. These are simply the calculation routines that are accessible to the outside world. A Foreign Object method in gPROMS calculates one quantity (the ”output”) for given values of one or more other quantities (the ”inputs”). Each gPROMS run may make use of any number of FOs, so there is the need to specify classes and instances. The class refers to the software used, as Multiflash or Microsoft Excel$^{\text{TM}}$, and the instance is related to the methods used in the calculation itself, as correlations and internal property data or different equations in different spreadsheets [21].

4.2.1 Foreign Object interface

The Foreign Object Interface (FOI) is the protocol used for communication between gPROMS and any external software component that provides services via one or more callable routines. A FO provides one or more methods, each of which takes inputs from gPROMS and returns an output. The inputs and output can be scalar or vector quantities. In addition to the value of the output, a FO method may also be able to provide values for the partial derivatives of its output with respect to one or more of its inputs.

Each FO class is implemented as a distinct piece of software. To achieve the required functionality, gPROMS makes use of six services provided by this software:

- FO instance initialisation procedure: gFOI;
- Two FO verification procedures: gFOCM, gFOCMI;
- Two FO calculation procedures: gFOM, gFOMD;
- FO string procedure (optional): gFOSTR;
- FO termination procedure: gFOT.

At the start of executing a Process entity, gPROMS will construct a list of all distinct FO classes and their instances that are used by it. It then attempts to create each instance by calling the gFOI procedure of the corresponding class. This procedure requires a string identifying the instance of the FO class that is to be created. The success or failure of the attempted instance creation must be reported to gPROMS via a Status argument. If the instantiation fails (Status different from 1), the execution of the Process cannot proceed further and is terminated immediately.

The verification procedure gFOCM is used by gPROMS to ascertain the existence of a given method, to determine the number of the inputs that the method expects, and to obtain detailed information on the method's output. Using the FO identification and the method name, gFOCM returns the number of inputs that this method expects as well as type and length of the method's output. The type can be integer, real, logical or string.

The next step is to obtain detailed information on the method's inputs. This is achieved via a call to the routine gFOCMI that provides the number, name, type and length of the inputs as well as flags that indicate whether the method can compute partial derivatives of its output with respect to its inputs.

If the Foreign Object initialisation and verification are completed successfully, gPROMS proceeds with the execution of the Process under consideration. This requires the evaluation of the outputs of the various Foreign Object methods used in the problem for given values of their inputs. It also usually involves the evaluation of partial derivatives of the outputs with respect to the inputs. The procedure gFOM takes the identifications of the FO and method, the output and inputs lengths and the inputs values to calculate the output of that method. gFOMD works in the same way but calculating a derivative of the output with respect to a specified input.

Strings are objects that represent a sequence of characters. An optional interface procedure gFOSTR allows implementing methods which are designated to return strings as output. This is essentially similar to the gFOM procedure except the method output parameter will be an array of strings of fixed length of 256.

At the end of the Process execution, gPROMS will call the termination procedure, gFOT, in turn for each FO instance that has been successfully created via an earlier successful call to gFOI. This is intended to provide the external package with an opportunity to do any necessary housekeeping (e.g. closing of databank files etc.).

Several of this above mentioned procedures require the definition of the lengths of both inputs and output and these values cannot depend on other inputs or calculations performed in gPROMS or the FO itself, they are fixed values *a priori* [22].

4.2.2 Implementation of Foreign Objects

As will be discussed in section 4.2.3, the language used to implement the FO in this project was C++. This implementation is divided in 3 main responsibilities:

- interface to gPROMS;
- managing the FOs, comprising the task of creating, destroying and accessing them;

- the Foreign Objects.

The classes and interfaces are provided by PSE and designed so that the user can use them as a library without having to bother with the low-level interface to gPROMS and the management of the FOs. In the above list, the second group of responsibilities is dealt with by a single object, a so-called Factory. On request, this Factory will create and destroy Foreign Objects. Internally it keeps track of all the Foreign Objects. Actually, the Factory is designed to be the only interface through which Foreign Objects can be created and accessed. Two additional classes are also provided: gFOClass and gFOFactory. Both of them are purely abstract classes, which means it is not possible to instantiate them directly. Instead, their purpose is to provide the basic functionality which has to be implemented in the Foreign Object. When defining and implementing a Foreign Object, the necessary classes should be derived from these two classes and virtual functions should be defined of the abstract base classes. In this context, gFOClass is the base class for the Foreign Object, whereas gFOFactory is the base class for a user-provided factory which is responsible for generating and accessing a single or multiple Foreign Objects.

When deriving from gFOClass, the only member functions which have to be provided by the user are the equivalents for the service procedures discussed above. Table 4.1 shows the C++ member functions equivalent to the service procedures.

Table 4.1: FO interface procedures and equivalents in C++ implementation.

Service procedures	**C++ equivalent**
gFOCM()	CheckMethod()
gFOCMI()	CheckMethodInputs()
gFOM()	EvalMethod()
gFOMD()	EvalMethodDeriv()

The only difference in arguments is that the member functions do not require the FO identification because they operate on the specific object with which they are associated. The Evalmethod function is the one that contains the calculations that transform the inputs in the method output [22].

4.2.3 C++

C++ is a general-purpose programming language that was used in this work. It has imperative, object-oriented and generic programming features, while also providing the facilities for low-level memory manipulation. C++ offers a straightforward way to implement a Foreign Object and to manage multiple instances of the same class. In principle, Foreign Object software can be written in any procedural language such as FORTRAN, C and C++. Although the first two are perfectly adequate, at least for simple applications, special care must be taken if the problem under consideration makes use of multiple instances of the same Foreign Object class [21].

The gPROMS “engine” that comprises the solvers is written in C++, which makes it easier to communicate to FOs also written in the same language. Besides, with this language it is also possible to get access to the “machine” itself when needed, which makes it a very performant language. For these reasons this was the language chosen to write the Foreign Object developed in the present work.

4.3 Multiflash package

There is no universal physical properties package that can supply all requirements. For this reason PSE’s approach is to provide a wide range of optional rigorous physical property packages that cater for different needs. In this work the property package used was Multiflash.

Multiflash is an advanced software package for performing complex equilibrium calculations quickly and reliably. The main utility is a multiple phase equilibrium algorithm that is interfaced to Infochem’s package of thermodynamic models and a number of physical property data banks [23].

Within the context of Multiflash, a model is a mathematical description of how one or more thermodynamic or transport properties of a fluid or solid will depend on pressure, temperature or composition.

The key thermodynamic property calculation carried out within Multiflash is the determination of phase equilibrium. This is based on the fundamental relationship that at equilibrium the fugacity of a component is equal in all phases. For a simple vapour-liquid system:

$$f^{v}_{comp} = f^{l}_{comp} \tag{4.1}$$

f^{v}_{comp} is the fugacity of component *comp* in the vapour phase and f^{l}_{comp} is the fugacity of component *comp* in the liquid phase.

The models used in Multiflash to represent the fugacities from the phase equilibrium relationship in terms of measurable state variables (temperature, pressure, enthalpy, entropy, volume and internal energy) fall into two groups: equation of state methods and activity coefficient methods. With an equation of state method, all thermal properties for any fluid phase can be derived from the equation of state. With an activity coefficient method the vapour phase properties are derived from an equation of state, whereas the liquid properties are determined from the summation of the pure component properties to which a mixing term or an excess term has been added.

Table 4.2: Multiflash methods used in this work.

Multiflash method	**Inputs**	**Description**
PHFlash	P, H, w	Equilibrium pressure and enthalpy flash
TPFlash	T, P, w	Equilibrium temperature and pressure flash
DewTemperature	P, w	Dew point temperature of the mixture
BubbleTemperature	P, w	Bubble point temperature of the mixture

Multiflash may also be used to calculate the phase equilibrium of systems containing solid phases, either mixed or pure. These may occur either when a normal fluid freezes or may be a particular solid phase such as a hydrate, wax or asphaltene. The transport properties of a phase (viscosity, thermal conductivity and surface tension) are derived from semi-empirical models [23].

In the models developed in this work, four different methods of the Multiflash software were used. Table 4.2 contains these methods description and inputs. P stands for pressure, H enthalpy, T temperature and w composition.

Chapter 5

Multi-stream heat exchanger model

This chapter contains a detailed description of the models developed in this work. A scheme of the global model that simulates the multi-stream heat exchanger can be seen in figure 5.1.

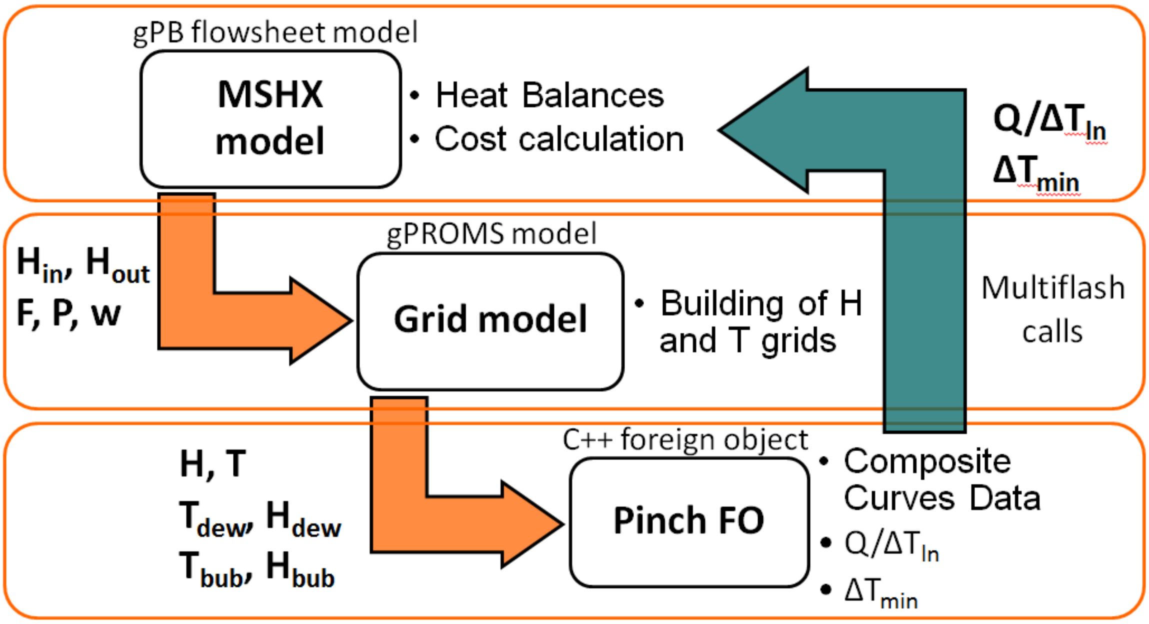
gPB flowsheet model
MSHX model
• Heat Balances
• Cost calculation
Q/ΔT$_{ln}$
ΔT$_{min}$
H$_{in}$, H$_{out}$
F, P, w
gPROMS model
Grid model
• Building of H and T grids
Multiflash calls
H, T
T$_{dew}$, H$_{dew}$
T$_{bub}$, H$_{bub}$
C++ foreign object
Pinch FO
• Composite Curves Data
• Q/ΔT$_{ln}$
• ΔT$_{min}$

Figure 5.1: Schematics of the global MSHX model.

This model has the purpose of simulating a MSHX including a tool to estimate its cost using the Pinch analysis algorithm. It is composed of 3 sub-models, 2 written in gPROMS language and one FO written in C++ as can be observed in figure 5.1. The upper level model (MSHX model in the figure) was adapted from an existing model of the ProcessBuilder libraries and the Grid model and Pinch FO were fully developed during the present work. The sub-model containing the Pinch algorithm was developed as a FO because this is a sequential method that involves vector and matrix manipulation using several intermediate variables.

The MSHX model calculates mass and heat balances providing the properties like enthalpy and temperature for all the inlets and outlets of the exchanger. The Grid model builds enthalpy and temperature grids for the streams and makes calls to the Pinch FO. The Multiflash calls occur in the gPROMs models, mainly in the Grid model, using Peng-Robinson equation of state to calculate the properties of the streams. The Pinch FO uses the Pinch algorithm to build the composite curves, calculate the mean logarithmic temperature difference (MLTD), the heat load for every stream in each interval (Q) and the minimum temperature approach between hot and cold streams (ΔT_{min}). The $Q/\Delta T_{ln}$ factor is then used to estimate the exchanger cost using the C value method in the MSHX model.

5.1 MSHX model

The heat_exchanger_multistream model represents a heat exchanger with more than two streams exchanging heat. Some thermal specifications are available, such as outlet temperatures, outlet pressures and pressure drop. The model calculates the heat lost by the hot streams and the heat received by the cold streams, as well as the temperatures and pressures of N-1 streams, being N the number of streams, figure 5.2. The model calculations are essentially heat balances stating that the total inlet enthalpy of all streams has to match the total outlet enthalpy, determining the heat transferred by each stream. The inputs of the model are represented in table 5.1.

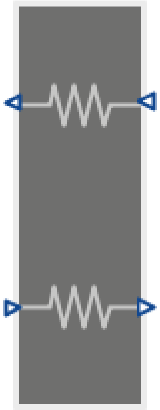

Figure 5.2: Topology representation of the heat_exchanger_multistream model.

Table 5.1: Inputs of the heat_exchanger_multistream model.

Input	Size	Variable type	Definition
T^{in}	N	Real	Inlet temperature
T^{out}	N-1	Real	Outlet temperature
P^{in}	N	Real	Inlet pressure
ΔP or P^{out}	N	Real	Pressure drop or outlet pressure
F	N	Real	Flowrate
w	N×*nc*	Real	Stream composition

This is a flowsheet model of the gML libraries of gPROMS ProcessBuilder and to be used in the scope of this work some options were added:

- Lower level model Grid as a new Unit;
- Design option to activate and deactivate the lower level model calculations;

- Connections between models' variables (upper and lower level);
- Composite curves in report;
- Correlation to estimate the exchanger cost.

In figure 5.1 the gML model with the appropriate changes is represented as MSHX model. The correlation used for the calculation of the exchanger cost is called C Value Method [24, 25] and is represented in equation 5.1. This method is grounded by equation 5.2 where F' is a correction factor that is 1 for counter-current heat exchange, U is the overall heat transfer coefficient and A the heat transfer area. This equation shows how UA is equivalent to $Q/\Delta T_{ln}$ in the heat balance equation. In this method, C is defined as the cost per unit of $Q/\Delta T_{ln}$. This avoids difficulties in defining area and heat transfer coefficients and allows a direct comparison between heat exchangers in terms of duty and available temperature driving force, which are related to the process specification. The determination of the $Q/\Delta T_{ln}$ factor is performed in the Pinch FO.

$$Cost = C \times \left(\frac{Q}{\Delta T_{ln}}\right) \tag{5.1}$$

$$Q = F' \times U \times A \times \Delta T_{ln} (=) F' \times U \times A = Q/\Delta T_{ln} \tag{5.2}$$

As in many other methods, this method considers "standard" values for film and overall heat transfer coefficients in heat exchangers. The heat transfer coefficients are strongly related to the available pressure drop but in process specifications the pressure drop tends to lie within a restricted range, so the coefficients are often also in a restricted range. The other constituent information required in establishing C values is the cost per unit area. The data to calculate C values in literature is obtained with the assistance of exchanger manufacturers and is based on actual cost data for a variety of exchangers. The C values used here, table 5.2, were taken from [26] for purposes of comparison as it is explained later on. The determination of the C value for other conditions is done by logarithmic interpolation as represented in equation 5.3.

Table 5.2: C values used in the correlation to estimate the MSHX cost [26].

C values	$Q/\Delta T_{ln}$ **(kW/K)**
0.392	100
0.222	1000

$$C = \exp\left\{ \ln C_1 + \frac{\ln\left(C_2/C_1\right) ln\left[\left(\frac{Q}{\Delta T_{ln}}\right) / \left(\frac{Q}{\Delta T_{ln}}\right)_1\right]}{ln\left[\left(\frac{Q}{\Delta T_{ln}}\right)_2 / \left(\frac{Q}{\Delta T_{ln}}\right)_1\right]} \right\} \tag{5.3}$$

C_1 and C_2 are the C values of the particular hot-side/cold-side fluid pairing at $(Q/\Delta T_{ln})_1$ and $(Q/\Delta T_{ln})_2$, respectively. The relative cost of one exchanger type against another varies with $(Q/\Delta T_{ln})$ but in this project this variation is not considered because the model is general in terms of design, which means it was not particularly developed to fit one type of exchanger geometry.

In Pinch analysis the heat transfer area is calculated for each enthalpy interval and the total area is estimated to be the sum all the intervals' areas, see equation 3.1. Similarly, C value is calculated for each stream in each interval, as well as $(Q/\Delta T_{ln})$ and the total cost is considered to be the sum of the costs of all the parcels, equation 5.4.

$$\text{Exchanger cost} = 1.25 \times \sum_i \sum_j C_{ji} \times \left(\frac{Q}{\Delta T_{ln}}\right)_{ji} \tag{5.4}$$

Later on, the global model is used in a case study flowsheet with high pressures and, according to [25], for pressures in the range between 60 and 80 bar, the cost should be multiplied by a factor of 1.25, equation 5.4, where j and i represent streams and intervals, respectively.

5.2 Grid model

The Grid model is responsible for the determination of the enthalpy and temperature grids that are required for the Pinch FO calculations. The inputs of the model are represented in table 5.3.

Table 5.3: Inputs of the Grid model.

Input	**Size**	**Variable type**	**Definition**
N	1	Integer	Number of streams
Z	N	Integer	Number of intervals to divide enthalpy ranges
H^{in}	N	Real	Inlet enthalpy
H^{out}	N	Real	Outlet enthalpy
P	N	Real	Pressure
F	N	Real	Flowrate
w	$N \times nc$	Real	Stream composition
$cond$	N	0/1	Info on condensable stream
vol	N	0/1	Info on volatile stream

H^{in}, H^{out}, $cond$ and vol are determined in the MSHX model and passed to the lower level model (Grid). nc is the number of components of the fluid, to which a composition is assigned by the user. Z is the number of intervals assigned by the user to each stream to divide its enthalpy range. This is done to implement a piecewise linearization of the enthalpy-temperature dependency. $cond$ and vol are arrays of binary numbers that indicate if a stream is condensable and volatile, respectively. These parameters are required because in many cryogenic processes, the streams are in the critical fluid stage and Multiflash may not be able to calculate the dew or bubble points causing the simulation to fail.

The Grid model takes the number of intervals for each stream, Z, as input and creates a set of enthalpy equidistant points from the inlet to the outlet enthalpy. These enthalpy sets are grouped in a grid being each row correspondent to a different stream. Then the matching temperature grid is built using a PHFlash call, see chapter 4.3. With these sets of points of calculated enthalpies and temperatures, it is viable to assume that in each interval (between two points) the enthalpy changes linearly with temperature, see chapter 3.1. Z may have a different value for each stream (array of size

N), however the grids need to have the same number of columns so the empty positions of the rows with less points are filled with zeros. The zeros introduced are recognised by the Pinch FO as having no physical meaning being used for numerical purpose only.

The dew and bubble temperatures are calculated using DewTemperature and BubbleTemperature calls and the correspondent enthalpies with TPFlash calls, see chapter 4.3. These will be inputs to the FO as well as the H and T grids. The enthalpy grid needs to be converted from units of specific enthalpy to units of power by multiplying each row by the correspondent stream flowrate and then it is passed to the Pinch FO. The outputs of this model are the inputs of the Pinch FO, represented in table 5.4, section 5.3.

5.3 Pinch FO

Each Foreign Object can contain several methods, as explained in chapter 4.2. The FO developed during this work includes two methods: **PinchMS** and **PinchUtilities**. Both methods make use of the Pinch algorithm being the only relevant difference the calculation of the utilities heat in the second one, that will be covered in section 5.3.2.

Both methods contain the Pinch algorithm that performs sequential matrix and array manipulation to build the composite curves and estimate the exchanger cost. The inputs and outputs of the method PinchMS are defined in tables 5.4 and 5.5, respectively.

Table 5.4: Inputs of the PinchMS method of the Pinch FO.

Input	Size	Variable type	Definition
H	$N \times M$	Real	Enthalpy grid
T	$N \times M$	Real	Temperature grid
$DewPoint$	$2 \times N$	Real	Dew point data
$BubblePoint$	$2 \times N$	Real	Bubble point data

Table 5.5: Outputs of the PinchMS method of the Pinch FO.

Output	Size	Variable type	Definition
ΔH_{ac}	$Sz + 1$	Real	Accumulated enthalpy (composite curves)
T_{HOT}	$Sz + 1$	Real	Hot curve temperature
T_{COLD}	$Sz + 1$	Real	Cold curve temperature
$Q/\Delta T_{ln}$	$N \times Sz$	Real	Duty over mean logarithmic temperature difference
ΔT_{min}	1	Real	Minimum approach temperature

N is the number of streams and M is the maximum number of points of the enthalpy sets defined in the Grid model, meaning it is the number of columns of the H and T grids, equation 5.5.

$$M = max(Z_j) \tag{5.5}$$

In the interface linking Foreign Objects to the gPROMS software the sizes of the inputs and output have fixed values that cannot be passed also as inputs to the FO. So N, M and the output size are passed to the FO via a text file implemented in the gPROMS project in use. Sz is the number of enthalpy intervals of the composite curves that result from the Pinch calculations.

The $DewPoint$ and $BubblePoint$ arrays store the dew and bubble temperatures and enthalpies of the streams, respectively. These were determined in the Grid model.

The minimum temperature approach between hot and cold streams, ΔT_{min}, is directly related to the effectiveness of the exchanger and will be used as optimisation constraint, chapter 6. The rest of the data returned from the PinchMS method is passed to the MSHX model where the composite curves are built and $Q/\Delta T_{ln}$ is used to estimate the cost of the exchanger.

As stated before, in chapter 4.2, each FO method has only one output, thus the outputs of the Pinch algorithm are stored in the form of one single array. In the Grid model the output array is again separated in different variables and to do this it is required that the size of these output variables is known *a priori*. Observing table 5.5 it is possible to identify that there is one size that is not known, the number of final intervals of the composite curves, Sz, that is the number of columns of matrix $Q/\Delta T_{ln}$. To use the global model in optimisation cases (chapter 6) the sizes of the FO's outputs need to be known before the calculations. Thus, Sz has to be a parameter of the Grid model, meaning it does not change with any calculation neither in the gPROMS models or in the Pinch FO.

To guarantee that Sz is fixed and only depending on the inputs of the gPROMS models there is the need of a special procedure in the calculations. This implies that when new points are introduced in a set of temperatures or enthalpies, the duplicates are never removed and when the dew and bubble points are not inside the range of a stream, dummy values are introduced to fill their spaces. The dummies are duplicates of other existing points that will not influence the results because 2 consecutive equal enthalpy points will produce a duty of 0. This way Sz is fixed depending only on the number of initial intervals Z (input of the Grid model) and it is calculated using equation 5.6.

$$Sz = \sum_{j} (Z_j + 1 + 2) - 1 - 1 \tag{5.6}$$

It is added 1 and 2 to the number of intervals of each stream (inside the summation). 1 because the number of points is one more than the number of intervals and 2 due to the spaces of the dew and bubble points, that are filled even when these are not inside the range as described in the text above. It is subtracted 1 because when the accumulated enthalpies of both curves are put together to divide the curves in enthalpy intervals, there are always 2 zeros (first position of accumulated enthalpy arrays is zero) thus one of the zeros can be always removed. Finally, -1 converts Sz from points to intervals again.

5.3.1 PinchMS algorithm

The steps followed by the algorithm of the PinchMS method are represented in figure 5.3.

Initially the streams are defined as hot or cold trough comparison of the first enthalpy point with the second because the grids enter the FO sorted from inlet to outlet enthalpy/temperature. This information is stored in a binary array at the beginning because in the following steps the sets of temperature and

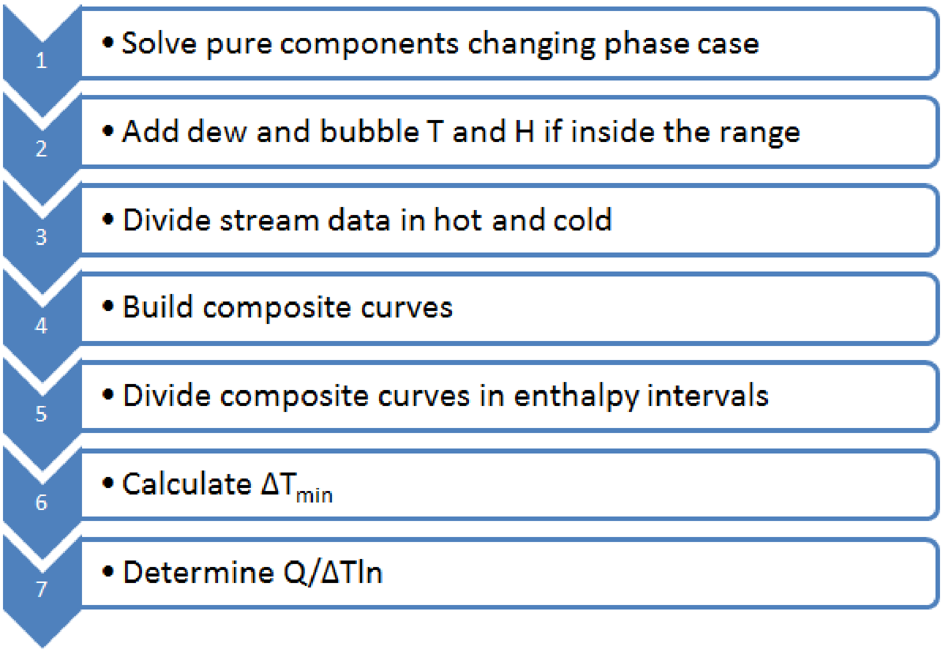
1
• Solve pure components changing phase case
2
• Add dew and bubble T and H if inside the range
3
• Divide stream data in hot and cold
4
• Build composite curves
5
• Divide composite curves in enthalpy intervals
6
• Calculate ΔT$_{min}$
7
• Determine Q/ΔTln

Figure 5.3: PinchMS algorithm list of steps.

enthalpy are sorted in a different way.

The first step of the list regards the possibility of a stream composed of a pure component changing phase in which case the temperature is constant while the enthalpy changes. This situation is not favourable for the calculations since the enthalpies of the streams will be summed for each temperature level. In the Pinch analysis this situation is usually dealt with a small temperature variation, δ. The duplicate temperatures are replaced by a range of equidistant points from $T-\delta$ to $T+\delta$ being the value of δ chosen of 0.1K. During this procedure the enthalpy and temperature rows are sorted in ascending order.

Step 2 is to introduce the dew and bubble points in the grids if they are inside the stream range (for both enthalpy and temperature sets). This improves the linearisation assumed for each interval as these are the points of more abrupt change in the curve temperature vs. enthalpy.

In step 3 the enthalpy and temperature grids are divided in hot and cold to facilitate the construction of the composite curves, hot and cold separately.

The hot and cold composite curves are built in parallel and in the same way, step 4, thus, only the hot curve is regarded in the following exposition. The temperature points of all hot streams are placed in one single array, $allT_{HOT}$, and the corresponding enthalpies are determined for all hot streams and placed in a new enthalpy grid, $allH_{HOT}$. The extra temperature points in $allT_{HOT}$ (compared to the points in the initial T grid) can be the same or different from the initial T set of the corresponding stream. If different they can be inside the range of the set or outside. For points that are the same, the enthalpy is also the same as in the initial H grid; for different points inside the range the enthalpies are determined by interpolation between two adjacent points of the initial H grid; for points outside the range, the first or last enthalpy values of the stream are assigned. If the temperature is smaller than the outlet temperature of the hot stream (first temperature of the set, inlet temperature for cold streams as the sets are arranged in ascending order), the corresponding enthalpy point is the first of the set. Similarly, if the temperature is higher than the last temperature of the stream range, it is assigned the last enthalpy to the correspondent point of the new grid. Figure 5.4 exemplifies this assignment method.

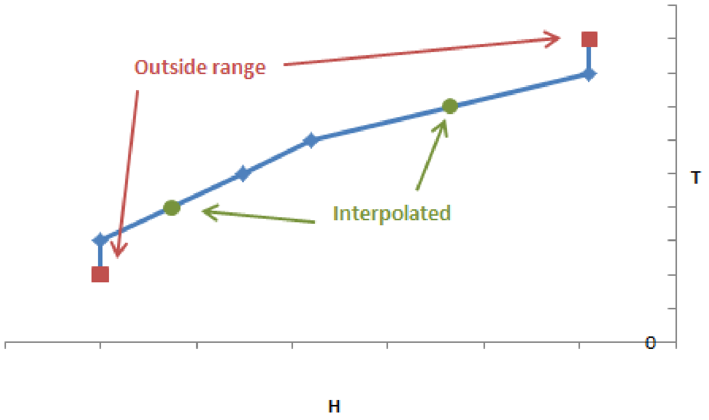

Figure 5.4: Assignment method used to complete new matrices or arrays.

In figure 5.4 the original range is represented in blue; in green the new points inside the range, determined by interpolation; and in red the points outside the range, to which the first/last value of the range is assigned. This way when the heat load of the interval is calculated, the contribution of a stream for temperatures outside its original range will be zero, meaning that stream does not exchange heat on that particular interval.

Then the enthalpies of all hot streams in each temperature level are summed, equation 5.7 where p and j represent points and streams, respectively, and H is the new enthalpy grid of hot streams built with the assignment method in figure 5.4.

$$SumH_p = \sum_j H_{jp} \tag{5.7}$$

So far all values where points of temperature and enthalpy. Next there is the calculation of the accumulated enthalpy, ΔH_{ac}, that refers to an interval, comprised by two consecutive points. ΔH_{ac} is calculated using equation 5.8 where i represents intervals and 1 corresponds to the first position of the array.

$$\Delta H_{ac,i} = SumH_p - SumH_1 \tag{5.8}$$

The hot composite curve is composed by pairs of enthalpy-temperature points where the enthalpy is the accumulated enthalpy in equation 5.8 and the temperatures are in the $allT_{HOT}$ array. The cold composite curve is calculated in parallel with the same procedure. The composite curves consist in a graphical combination of all hot and cold process streams in the heat exchange process.

In step 5 the composite curves are further divided in enthalpy intervals so that in each interval none of the curves changes slope, as explained in chapter 3, see figure 3.3. The ΔH_{ac} array is then completed to contain all enthalpy points of both composite curves and becomes $areaH$. The completion of the temperature arrays $areaT_{HOT}$ and $areaT_{COLD}$ to correspond to the enthalpy points in $areaH$ is done with the assignment method explained above, figure 5.4. The resulting composite curves, constituted by the data contained in the arrays $areaT_{HOT}$, $areaT_{COLD}$ and $areaH$, are represented in figure 5.5. In step 6 the difference between hot and cold temperatures is calculated for all the points of the curves and ΔT_{min} is identified.

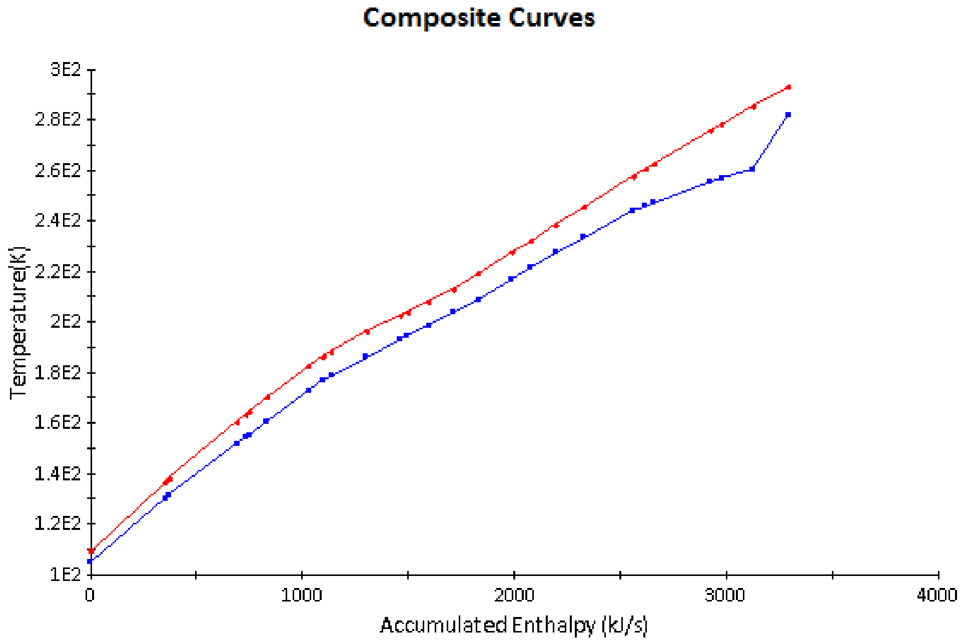

Figure 5.5: Composite curves representation.

Step 7 comprises the calculation of the remainder output of the method. Using the new temperature arrays $areaT_{HOT}$ and $areaT_{COLD}$, the MLTD is calculated as in counter-current heat exchange, see figure 5.6.

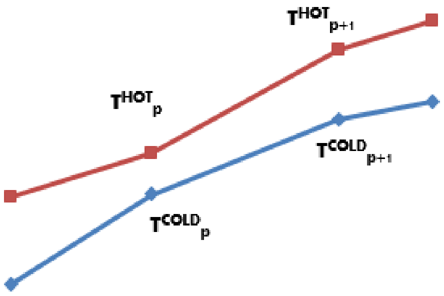

Figure 5.6: Demonstration of counter-current ΔT_{ln} determination with p representing points. The hot curve is flowing to the left while the cold curve is flowing to the right but both curves' arrays are ordered in ascending order.

Equation 3.2 is converted to equation 5.9 to be used in the Pinch algorithm. When the difference between hot and cold temperatures of two consecutive points is the same, ΔT_{ln} is calculated using equation 5.10 [15].

$$\Delta T_{ln} = \frac{(T_{HOT}^{p+1} - T_{COLD}^{p+1}) - (T_{HOT}^{p} - T_{COLD}^{p})}{ln\left[\frac{(T_{HOT}^{p+1} - T_{COLD}^{p+1})}{(T_{HOT}^{p} - T_{COLD}^{p})}\right]} \tag{5.9}$$

$$\Delta T_{ln} = T_{HOT}^{p+1} - T_{COLD}^{p+1} \tag{5.10}$$

A multi-stream heat exchanger only exchanges heat between the streams that pass through the unit and does not consume any hot or cold utilities. However, during optimisation runs with the Pinch model, the process can be simulated with infeasible conditions that would require utilities to close the heat balance, the consequence being temperature crossing. A temperature cross refers to the case when the cold fluid temperature becomes equal or greater than the hot fluid temperature within the exchanger. This indicates a negative driving force for heat transfer between the fluids so it requires either a larger area or greater fluid velocity to increase overall heat transfer coefficient. The temperature cross is undesirable because the area is not utilised effectively and hence there is a wastage of capital cost but some engineers suggest that a small temperature cross may be acceptable and may provide a less expensive design than the more complex alternatives used to solve it [27].

To prevent the simulation from failing during the search for the optimum conditions, the model allows the cross in temperature by recognising such situations and calculating the MLTD accordingly: the curves are inverted on such intervals, thus the logarithmic temperature difference is calculated using equation 5.11.

$$\Delta T_{ln} = \frac{(T_{COLD}^{p+1} - T_{HOT}^{p+1}) - (T_{COLD}^{p} - T_{HOT}^{p})}{ln\left[\frac{(T_{COLD}^{p+1} - T_{HOT}^{p+1})}{(T_{COLD}^{p} - T_{HOT}^{p})}\right]} \tag{5.11}$$

Finally, there is only left to calculate a matrix with the streams duty. Taking the arrays $areaT_{HOT}$ and $areaT_{COLD}$ from the composite curves division, the correspondent enthalpies are calculated for each stream with the assignment method mentioned before, using and interpolating values from the initial enthalpy grid. The resulting grid is $auxH$ that includes both hot and cold streams enthalpy points. By calculating the difference between the heat of two consecutive points of this matrix, the duty matrix Q is obtained. Q represents the heat transferred by each stream in each enthalpy interval of the composite curves. At last, Q is divided by the mean logarithmic temperature difference of the interval and passed to the MSHX model as $Q/\Delta T_{ln}$ to be used in the estimation of the cost of the exchanger.

The outputs of the PinchMS method are passed to the Grid model and there are then divided to form the individual variables that are finally passed to the MSHX model.

5.3.2 PinchUtilities method

The PinchUtilities method of the Pinch FO regards utility consumption. This can be applied to a network of simple heat exchangers. This method was not used in optimisation because in the presented case the use of utilities is not required but it complements the Pinch FO for future use in other applications.

The inputs and outputs of the method are stated in tables 5.6 and 5.7. In fact the method returns only one array with the output data that is then divided in different variables in the upper level model, as in the PinchMS method.

Table 5.6: Inputs of the PinchUtilities method of the Pinch FO.

Input	**Size**	**Variable type**	**Definition**
H	$N \times M$	Real	Enthalpy grid
T	$N \times M$	Real	Temperature grid
$DewPoint$	$2 \times N$	Real	Dew point data
$BubblePoint$	$2 \times N$	Real	Bubble point data
ΔT_{min}	1	Real	Minimum temperature approach
UtT	4	Real	Utility temperatures

Table 5.7: Outputs of the PinchUtilities method of the Pinch FO.

Output	**Size**	**Variable type**	**Definition**
ΔH_{ac}	$Sz + 1$	Real	Accumulated enthalpy (composite curves)
T_{HOT}	$Sz + 1$	Real	Hot curve temperature
T_{COLD}	$Sz + 1$	Real	Cold curve temperature
Q	$N \times Sz$	Real	Heat duty
ΔT_{ln}	Sz	Real	Mean logarithmic temperature difference
Q_{HU}	1	Real	Hot utility heat
Q_{CU}	1	Real	Cold utility heat

Many of the inputs and outputs are common to the PinchMS method and the calculations are also similar, thus only the different parts will be covered in this explanation. Instead of moving the composite curves closer together to satisfy the total process heat transfer (meaning the total heat provided by the hot streams is received by the cold streams, no utilities involved) like in the first method, in this case it is the minimum temperature difference, ΔT_{min}, that constrains this movement of the composite curves and that is why ΔT_{min} is given as input. The other new input is an array with the inlet and outlet temperatures of both hot and cold utilities, UtT, that can be chosen by the user according to the process being considered. Regarding the outputs, the heat duties and the MLTD are given in separate to allow for the calculation of the area using heat transfer coefficients calculated in gPROMS, like in equation 3.1. This is just to show the flexibility of the calculation routines as the cost can be calculated using the area or directly using the C value method as in the first method. The scheme of the PinchUtilities method is presented in figure 5.7.

The calculation of the utilities heat required for the process is done with the Heat Cascade or Problem table[15], step 5. First, the shifted temperatures are calculated using equations 5.12 and 5.13.

$$T'_{COLD} = T_{COLD} + \frac{\Delta T_{min}}{2} \tag{5.12}$$

$$T'_{HOT} = T_{HOT} - \frac{\Delta T_{min}}{2} \tag{5.13}$$

T_C and T_H are the temperatures and T'_C and T'_H are the shifted temperatures of the cold and hot streams, respectively. The definition of these shifted temperatures guarantees that in any temperature

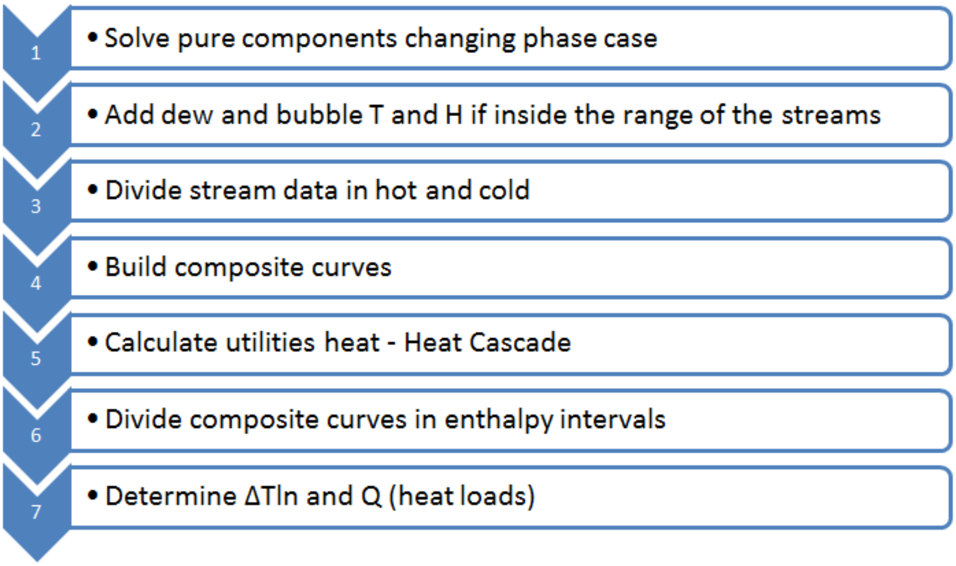
1
• Solve pure components changing phase case
2
• Add dew and bubble T and H if inside the range of the streams
3
• Divide stream data in hot and cold
4
• Build composite curves
5
• Calculate utilities heat - Heat Cascade
6
• Divide composite curves in enthalpy intervals
7
• Determine ΔTln and Q (heat loads)

Figure 5.7: Calculation steps of the PinchUtilities method.

interval the temperatures of the hot and cold streams are different in at least ΔT_{min}. Then it is made a heat balance to each interval defined by the shifted temperatures. This procedure is similar to that of the composite curves: gathering all the temperatures in one array, but in this case all hot and cold together, and get the respective enthalpies for every stream. The heat of an interval is then calculated using equation 5.14.

$$Q_i = \Delta H_{HOT,i} - \Delta H_{COLD,i} \tag{5.14}$$

Q_i is the heat of the interval and ΔH is the heat of the interval calculated for hot and cold streams. Finally the heat cascade is made, in a first stage by assuming zero hot utility and propagating the values of Q_i to all intervals, equation 5.15. As it is not possible to transfer heat from an inferior thermic level to a superior level, as negative accumulated enthalpies (ΔH_{ac}) suggest, the most negative value of ΔH_{ac} is added to the cascade in a correction stage. After correction, the first and last values of the cascade represent the hot and cold utility requirements, respectively.

$$\Delta H_{ac,i+1} = \Delta H_{ac,i} - Q_i \tag{5.15}$$

The composite curves are only complete when they have the representation of the utilities heat. The cold curve moves horizontally by Q_{CU} (cold utility heat) to meet the ΔT_{min} specification.

After the utilities heat calculation, the temperatures of the utilities are introduced in the $allT_{HOT}$ and $allT_{COLD}$ arrays as extra points and then the composite curves are divided in enthalpy intervals. Equation 3.1 is used to calculate the total heat transfer area calculating the heat transfer coefficients of all the process streams and also of the utilities in gPROMS. The heat exchange between process streams and utility streams can be distinguished in the duty matrix Q when the total heat of the hot streams is different from the total heat of the cold streams in a certain interval.

5.3.3 Algorithm validation

Validation of the model with experimental data is not presented in this work because it is very difficult to find public data. Thus, a validation of the model is done by comparison with another similar software in order to verify the accuracy of the calculations.

The Pinch model was then validated against a software that is also based on Pinch Analysis. Hint is a heat integration software used for heat exchanger network design that includes energy and cost targeting, utilities selection and network specification and optimisation through Pinch Analysis [28]. A simple gPROMS flowsheet model including only a MSHX with 3 streams with the required sources (entries) and sinks (exits) was built and data from a LNG flowsheet was used in the simulation. The results were compared with the result of the Hint simulation for the same input data which resulted in a perfect match. This validation simply verifies that the algorithm calculations are correct. It is to be noticed that it is proven that the Pinch Analysis method can be used to determine the heat transfer area within 10% of the actual minimum [17], so it can be inferred that the model has a good accuracy in terms of area prediction.

5.3.4 Computational complexity

Algorithm complexity is something designed to compare two algorithms at the idea level — ignoring low-level details such as the implementation programming language, the hardware the algorithm runs on, or the instruction set of the given CPU. As algorithms are programs that perform just a computation, and not other things computers often do such as networking tasks or user input and output, complexity analysis measures how fast a program is when it performs computations. Complexity analysis is also a tool that allows to explain how an algorithm behaves as the input grows larger. In practical programming, this is important as it makes possible to predict how the algorithm will behave when the input data becomes larger[29].

The purpose of the implementation of the Pinch algorithm in the calculation of the exchanger cost was to decrease the simulation time during optimisation of LNG flowsheets, as it is explained in chapter 6. In the reference case[26] used to compare the optimisation, chapter 6, there is a MSHX detailed model that is used in optimisation already but results in high optimisation times which is not desirable as the purpose of simulation and optimisation is to save time (and money). The speed of the Pinch FO computations depends highly on the number and size of inputs, thus the complexity analysis is important to improve this speed during the writing of the algorithm and to identify the parts of the code that have higher impact in this speed.

To facilitate the understanding of this analysis it is defined a mathematical function f(n) that, given the input size, n, gives back the number of instructions the algorithm needs. Sometimes the number of instructions of a certain piece of code does not depend solely on n but also on the input values which makes the definition of f more difficult. In this case it is usually considered the worst-case scenario. Given a single simple function it is easy to count the number of instructions but for more complex functions it becomes a tedious task. Besides, the number of actual CPU instructions needed for each programming language statement depends on the compiler of the programming language used and on the available CPU instruction set. Thus the function f goes trough a filter that removes terms that grow slowly and keeps the ones that grow faster as the size of inputs becomes larger. This filter is called asymptotic behaviour because it describes the performance of the algorithm in response to a ramp in the input size, and the filtered function f(n) is the asymptotic complexity[29].

A complexity analysis was performed on the Pinch algorithm and the slowest part of the code was identified, corresponding to the greatest complexity. This happens at the end of the Pinch algorithm in the calculation of the enthalpy matrix $auxH$, see section 5.3.1. The asymptotic complexity of this piece of code is $N^2 \times M \times \log M$ and comes from the use of the function *createInterpol* called inside a loop running the number of streams. The complexity of this function is $N \times M \times \log M$ because it contains search template functions inside a loop that runs $N \times M$ times. This loop is actually running the vectors $allT_{HOT}$ and $allT_{COLD}$ that contain all the temperatures of all the streams thus with size $N \times M$. The template functions use binary search that result in a complexity of log(n) being n the length of the vector where the search occurs, in this case being M, the size of the initial temperature/enthalpy sets from the Grid model. The conclusion is that when N and M increase, the Pinch FO computation time increases with the asymptotic complexity of $N^2 \times M \times \log M$.

5.3.5 Derivatives calculation

The Pinch algorithm is a sequential method with several intermediate variables and calculations that depend on the distribution of the values inside each intermediate array. For this kind of algorithm there is no simple function to describe it thus it is difficult to determine analytical derivatives. During optimisation with the NLPSQP solver the derivatives of the output with respect to each input of the method are required to determine the gradients that decide which direction must every decision variable take during optimisation.

gPROMS ProcessBuilder has the ability of calculating numerical derivatives for Foreign Objects that do not possess this option. Although, during the application of the model in an optimisation case, the gradients were not being correctly calculated which raised the necessity of this calculation in the Pinch FO itself. For this, numerical derivatives are determined for the PinchMS method simply by perturbing the inputs on both directions and determining the direction of the output regarding those perturbations, equation 5.16. The input variable x is perturbed and the output response is returned in f'.

$$f'(x) = \frac{f(x+\delta) - f(x-\delta)}{2\delta} \tag{5.16}$$

Derivatives with respect to inputs that are 0, like the values to fill the enthalpy and temperature grids for streams with smaller number of initial intervals and when bubble and dew points cannot be calculated by multiflash, are stated to be 0. The same happens for derivatives of outputs that are always 0, like the first value of the accumulated enthalpies of the composite curves. This direct assignment of zeros saves the computation time of those specific derivatives.

Chapter 6

Single-stage Mixed Refrigerant process optimisation

The purpose of the heat exchanger model developed in the present work was to be accurate but simple enough to be integrated in LNG flowsheets and result in fast optimisations. To verify this, the model was compared to another MSHX model in terms of optimisation time of a Single-stage Mixed Refrigerant (SMR) flowsheet with a multi-stream exchanger.

This chapter includes a brief explanation of the process that was optimised, the reference case used for the comparison, as well as the optimisation problem formulation including objective function, decision variables and constraints. The results of the initialization and of the optimisation case are presented and compared to the reference case, as well as the optimisation time.

6.1 SMR process

The base case used in optimisation was a PRICO process (see section 2.3.4) using a SMR cycle. The gas peak shaving plant is a technical alternative to compensate uncovered demand of natural gas in winter. As in all LNG plants, the main investment of this plant is in the natural gas liquefaction process where the sweet NG is fully condensed by using a refrigeration system along with special heat exchangers. This process is very energy consuming. The important equipment used here are compressors for circulating the refrigerant, compressor drivers and the heat exchangers for cooling and liquefying the NG and indeed exchanging heat between streams of refrigerant. The model developed in this project was used to simulate the main cryogenic heat exchanger in the gPROMS flowsheet of the SMR process in figure 6.1.

This flowsheet was assembled and optimised by Joungho Park during his MSc work at Imperial College [26]. During his project he worked closely with PSE consultants and his work was used in the present project to compare the time of optimisation of the SMR process when using the Pinch model or another MSHX model described in chapter 6.2.1. The reference work [26] was purely used for terms of time comparison and in the next sections of this chapter it is well defined what results are from the

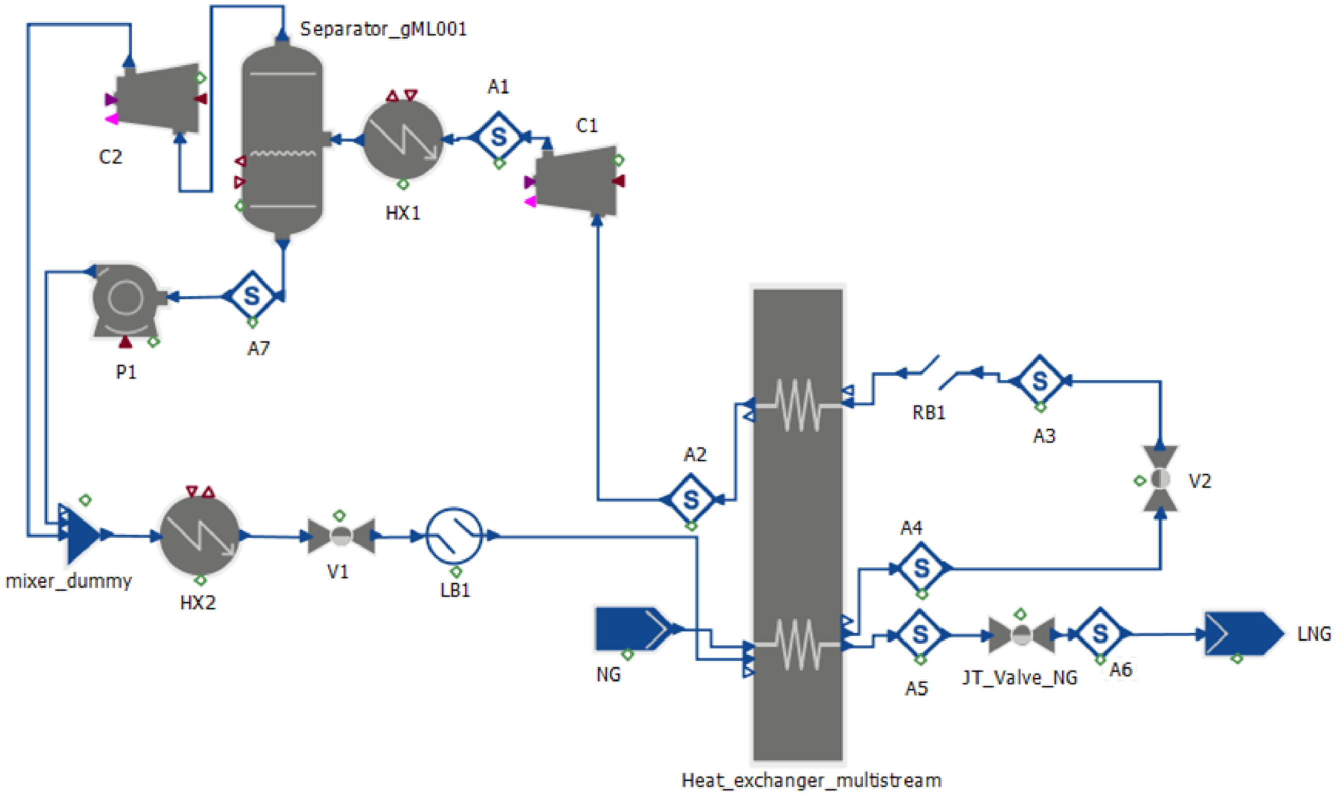
Separator_gML001
C2
A1
C1
HX1
A7
P1
RB1
A3
A2
V2
A4
mixer_dummy
HX2
V1
LB1
NG
A5
JT_Valve_NG
A6
LNG
Heat_exchanger_multistream

Figure 6.1: SMR process used in optimisation.

reference case and what results are from the work presented in this thesis. It should be kept in mind that the main purpose of this work is the design of a simple exchanger model that would allow for fast optimisation while maintaining an appropriate cost estimation.

In this process there are 3 streams going through the MCHX: 2 hot and 1 cold. The heated stream of MR leaves the exchanger and goes through a compression stage with inter-cooling where its pressure increases. Then this stream enters the MCHX as hot stream where it will be cooled and then suffers an expansion to reach the cooling power necessary to reenter the MCHX and liquefy the natural gas stream.

6.2 Reference case model

The reference case optimised the SMR process represented in figure 6.1 with a different cryogenic exchanger model than the one developed in this work. This chapter describes that heat exchanger model and the economic section included in the SMR flowsheet model.

6.2.1 Reference case heat exchanger model

The multi-stream heat exchanger model used in the reference case [26] was developed by PSE in gPROMS as a ”box” including 3 channels to represent the 3 streams of the process and 2 walls to represent the heat transfer between hot streams and cold stream. The channels make use of gPROMS library (gML) models called channel_1D_ gML and the walls are simulated by wall_1d_ gML. The energy balance for the channel is given by equations 6.1 to 6.3 and the notation of the variables is in table 6.1.

$$\frac{\partial \tilde{u}_{tube}(z)}{\partial t} + \frac{\partial q_{tube}(z)}{\partial z} = \frac{Q_{tube-tube,w}}{LA^{cross}_{tube}}, \quad \forall z \in (0, L] \tag{6.1}$$

$$\tilde{u}_{tube}(z) = \tilde{m}_{T,tube}(z)h_{tube}(z) - 10^2 P_{tube}(z), \quad \forall z \in [0, L] \tag{6.2}$$

$$q_{tube}(z) = N_{T,tube}(z)h_{tube}(z), \quad \forall z \in [0, L] \tag{6.3}$$

The boundary condition at the inlet and the outlet enthalpy are given by equations 6.4 and 6.5 respectively.

$$h_{tube}(z) = h^{in}_{tube}, \quad z = 0 \tag{6.4}$$

$$h^{out}_{tube} = h_{tube}(z), \quad z = 1 \tag{6.5}$$

Table 6.1: Notation of the variables in reference case model heat balance.

Variable	**Notation**
$\tilde{u}_{tube}(z)$	Volumetric energy holdup in the tube (kJ/m^3)
$q_{tube}(z)$	Tube energy flux (kJs^{-1}m^{-2})
$h_{tube}(z)$	Tube mass specific enthalpy (kJ/kg)
$P_{tube}(z)$	Tube pressure (bar)
$Q_{tube-tube,w}$	Heat duty transferred from the fluid to the tube wall (kW)
h^{in}_{tube}	Tube inlet mass specific enthalpy (kJ/kg)
h^{out}_{tube}	Tube outlet mass specific enthalpy (kJ/kg)

In short, the reference case model takes the areas of NG and MR sides and the number of intervals to divide the channels and performs heat balances in each interval resulting in the heat transferred and temperature profiles along the channels.

6.2.2 Process economics

To optimise the SMR flowsheet it was necessary to decide what costs to consider in the overall capital cost of the plant, select capital costs amortisation type and duration and decision factors as year of operation. This economic section was also included in the flowsheet provided in the reference case [26] and it will be described in this section to better elucidate the optimisation problem.

The technique used in the estimation of the profitability of the SMR process was the Net Present Value (NPV), defined as the present value of the future net cash flows from an investment project. The factor multiplied by the cash flows allows for the update of the currency amount to the year of the cash flow. The NPV formula for multiple investments is:

$$NPV = \sum CF/(1+r)^t \tag{6.6}$$

Where *CF* is a one-time cash flow, *r* is the discount rate and *t* is the time of the cash flow. For this project the discount rate used was of 15%. The cash flows were calculated from year -3, the beginning of the planning and construction stage, until year 0, the year when the plant operation starts, and then until year 15 considering this to be the end of the lifetime of the project. Figure 6.2 shows an example of the economic items involved during the whole life of a project.

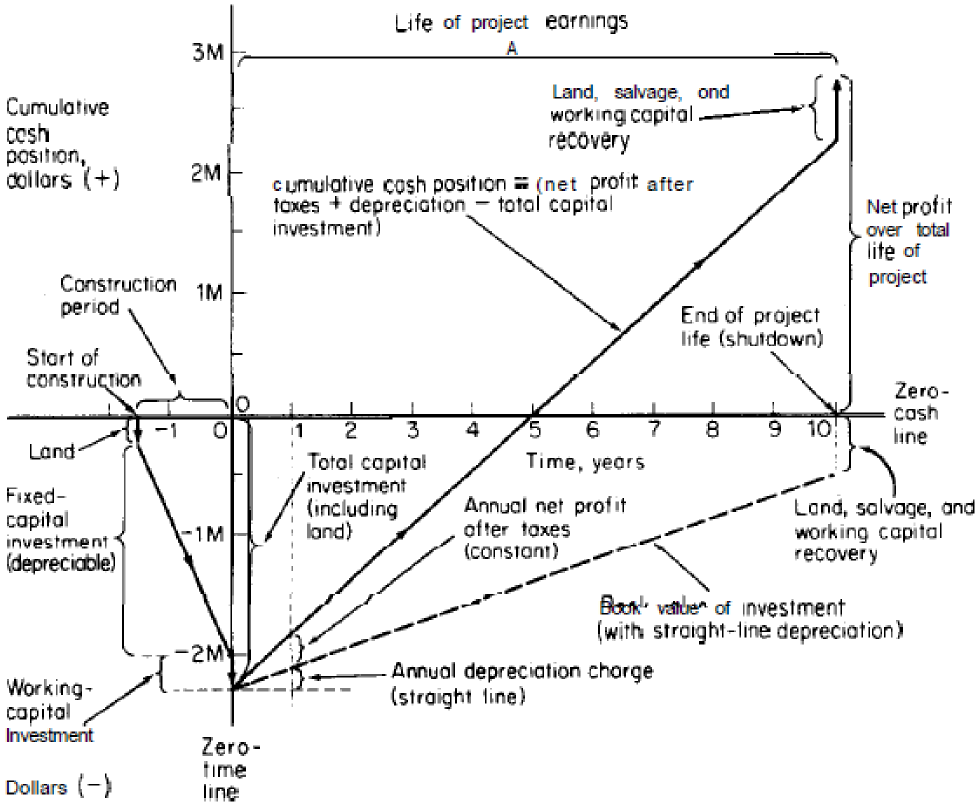

Figure 6.2: Economic items involved in the life of a project [30].

The zero point on the abscissa represents that time at which the plant has been completely constructed and it is ready for operation. The total capital investment at the zero point in time includes land value, fixed-capital and auxiliaries investment, and working capital. The cash position is negative by an amount equivalent to the total capital investment at zero time, but profits in the ideal situation come in from the operation as soon as time is positive. Cash flow to the company, in the form of net profits after taxes and depreciation charges, starts to accumulate and gradually pays off the full capital investment. For the conditions shown in figure 6.2, the full capital investment is paid off in five years. After that time, profits accumulate on the positive side of the cumulative cash position until the end of the project life at which time the project theoretically is shut down and the operation ceases.

For the years of planning and construction -3 to -1 of the SMR process the total annual cash flow corresponds to the negative fixed-capital cost (*FCI(year)*) and the total annual cash flow of year 0 is the negative sum of FCI(0) for year 0 and working capital, see equations 6.7 to 6.9.

$$\text{Total annual } CF(-2) = -FCI(-2) \tag{6.7}$$

$$\text{Total annual } CF(-1) = -FCI(-1) \tag{6.8}$$

$$\text{Total annual } CF(0) = -[FCI(0) + WC(0)] \tag{6.9}$$

The capital needed to supply the necessary manufacturing and plant facilities is called the fixed-capital investment, *FCI*, while that necessary for the operation of the plant is termed the working capital, *WC*. The sum of the fixed-capital investment and the working capital is known as the total capital investment. The calculations of the fixed-capital costs depend on the fraction of the *FCI* of the relevant year and the construction inflation rate, equations 6.10 to 6.12.

$$FCI(-2) = FCI \times 0.15 \times (1 + CIF)^0 \tag{6.10}$$

$$FCI(-1) = FCI \times 0.35 \times (1 + CIF)^1 \tag{6.11}$$

$$FCI(-2) = FCI \times 0.50 \times (1 + CIF)^2 \tag{6.12}$$

The investments are made over a period of time. This is represented on the basis that start-up (time 0) will be 3 years after the date of the estimate; that 15% of the fixed capital investment is spent in the beginning at the time of the estimate (year ending at time -2); 35% in the second year (ending at -1); and 50% in the third year (ending at time 0). The amounts are inflated at the beginning of each year after the estimate, by the default construction inflation rate, *CIF*. It is also assumed that all working capital is spent at time 0. The *WC* for year 0 was calculated with equation 6.13.

$$WC(0) = \frac{WC \times TCI}{FCI} \tag{6.13}$$

$$TCI = FCI(-2) + FCI(-1) + FCI(0) \tag{6.14}$$

TCI is the total capital investment, equation 6.14, that constitutes the sum of the *FCI* for all the years of the initial project stage. Both *FCI* and *WC* are obtained as percentages of the delivered equipment, *DE*, according to the method called Percentage of Delivered-Equipment Cost. *WC* was accounted as 89% of the Delivered Equipment. The *FCI* portion may be further subdivided into direct and indirect costs. To the direct costs it was assumed 260% of *DE* (excluding the equipment cost) that represents the capital necessary for the installed process equipment with all auxiliaries that are needed for complete process operation like expenses for piping, instruments, insulation, electrical systems, buildings, yard improvements and service facilities installation. The indirect costs account for 144% of *DE* in total, regarding all plant components that are not directly related to the process operation, such as engineering and supervision, construction and legal expenses, contractor's fee and contingency. Regarding the Total annual *CF* for the operation years it is correspondent to the annual operating cash flow, *OCF*, and this adds the depreciation to the net profit, see equations 6.15 and 6.16.

$$\text{Total annual } CF(i) = OCF(i), \quad \text{with } y = 1, ..., 15 \tag{6.15}$$

$$OCF(i) = D(i) + NP(i), \quad \text{with } y = 1, ..., 15 \tag{6.16}$$

Where *NP* is the annual net profit, *D* is the annual depreciation obtained using the Modified Accelerated Cost Recovery System (MACRS) with a five-year class as a percentage of *TCI* and *y* is the year to which these parcels refer to. The percentages of *TCI* used to calculate *D* from year 1 to 6 were 20, 32, 19.2, 11.5, 11.5 and 5.8% respectively. It was considered that from year 7 to 15 the annual depreciation would be 0. Depreciation represents the loss of value of equipment and facilities along the years due to use and technical progress. The net profit corresponds to the gross profit after taxes, equation 6.17.

$$NP(i) = GP(i) \times (1 - tr), \quad \text{with } y = 1, ..., 15 \tag{6.17}$$

GP is the annual gross profit, calculated with equations 6.18 and 6.19, and *tr* is the tax rate with the value of 35%. The gross profit results of the subtraction of the sales (S) with the production costs (TPC). In the way *TPC* was calculated the negative contribution is already included so TPC is summed to the sales. Depreciation is subtracted here and added after the taxes in equation 6.16.

$$GP(1) = S(1) + TPC(1) - D(1) - StartupCost \tag{6.18}$$

$$GP(i) = S(i) + TPC(i) - D(i), \quad \text{with } y = 2, ..., 15 \tag{6.19}$$

The Start-up Cost is calculated as 10% of the *TCI* for the first year only when the plant operation starts. Sales are calculated using a five-year (2010-2014) price average for LNG in the USA regarding LNG annual production, equations 6.20 to 6.22. For the first 2 years of operation the occupancy rate, *or*, is considered to be only 50 and 90% of the total capacity, respectively. In the rest of the years the plant works with its full capacity.

$$S(1) = \text{LNG price average} \times \text{LNG amount} \times 0.5 \tag{6.20}$$

$$S(2) = \text{LNG price average} \times \text{LNG amount} \times 0.9 \tag{6.21}$$

$$S(i) = \text{LNG price average} \times \text{LNG amount} \times 1, \quad \text{with } y = 3, ..., 15 \tag{6.22}$$

TPC includes variable, *VC*, and product costs, *PC*. In turn *PC* can be divided in Variable Costs, fixed charges, *FC*, plant overhead costs, *POC* and general expenses, *GE*.

$$TPC(i) = [VC \times (1 - or) - PC] \times (1 + CIF)^{i+2}, \quad \text{with } y = 1, ..., 15 \tag{6.23}$$

The variable costs include raw materials, operating and supervision labour, utilities, maintenance and repairs, operating supplies, laboratory charges and patents and royalties. Similarly to the sales calculation, the raw materials cost is calculated with a price assumed to be a five-year (2010-2014) average price of NG in the USA, equation 6.24. For the annual operating labour cost, *OLC*, it was assumed 3 workers per shift with 3 shifts of 8h each day for 365 days a year and an operator rate of 30.48$/h per worker. For the utilities cost it was considered the electricity and the cooling water cost. The electricity accounted for was the one used in the compressors at a price of 0.07$/kW and the cooling water used in the coolers of the process, costing 0.12$/m^3.

$$\text{Annual cost raw material} = \text{NG price average} \times \text{NG amount} \tag{6.24}$$

The rest of the contributions for the variable costs are calculated as percentages of other costs, see table 6.2.

Table 6.2: Variable costs constituents and respective contributions.

Item	**Fraction (%)**	**Basis**
Operating supervision	15	OLC
Maintenance and repair	6	TCI
Operating supplies	15	Maintenance and repair
Laboratory charges	15	OLC
Patents and royalties	1	PC

FC includes local taxes and insurance, *POC* accounts for medical services, general plant maintenance and overhead, safety services, payroll overhead including pensions, social security, employers' insurances, etc. and *GE* covers administration, distribution and marketing, and research and development expenses.

An extra 10% of the equipment cost was considered for delivery so the delivered equipment, *DE*, was calculated as 110% of the purchased equipment. The purchased equipment includes 2 compressors,

Table 6.3: Fixed costs constituents and respective contributions.

Item	Fraction (%)	Basis
Local taxes	2	FCI
Insurance	1	FCI
Plant overhead costs	60	Labor, supervision and maintenance
Administration	20	Labor, supervision and maintenance
Distribution & Marketing	5	PC
Research & Development	4	PC

main cryogenic heat exchanger, pump, separator and 2 coolers. Only the cost of the compressors and cryogenic exchanger were not assumed constant, depending on compressor power and $(Q/\Delta T_{ln})$, respectively.

The compressors cost was calculated using correlations for centrifugal compressors, equation 6.25, and turbines, equation 6.26. The pump cost calculation is stated in equations 6.27 to 6.29 and equations 6.30 to 6.32 were used to estimate the separator cost. All this cost correlations mentioned above were also included in the SMR flowsheet model and were taken from [31].

$$\text{Compressor cost (k\$)} = 7.90(HP)^{0.62} \tag{6.25}$$

$$\text{Turbine cost (k\$)} = 0.378(HP)^{0.81} \tag{6.26}$$

$$\text{Pump cost (\$)} = F_M F_T C_b \tag{6.27}$$

$$C_b = 3.00 \times exp[8.833 - 0.6019(lnQ_v\sqrt{H'}) + 0.0519(lnQ_v\sqrt{H'})^2] \tag{6.28}$$

$$F_T = exp[5.1029 - 1.2217(lnQ_v\sqrt{H'}) + 0.0771(lnQ_v\sqrt{H'})^2] \tag{6.29}$$

$$\text{Separator cost (\$)} = F_M C_b + C_a \tag{6.30}$$

$$C_b = 1.672 \times exp[9.100 + 0.2889(lnW) + 0.04576(lnW)^2] \tag{6.31}$$

$$C_a = 480D^{0.7396}L^{0.7066} \tag{6.32}$$

HP is the power of the compressor in Horse-Power. The correlation used for the pump regards a centrifugal pump with a base in cast-iron. F_M is the cost factor and it was selected the value of 2 for stainless steel 304 or 316. The values selected for F_T are related to a single-stage pump with 1750 rpm of speed. For the pump cost it was considered constant values for volumetric flowrate, Q_v = 10 m^{3}h^{-1}, and suction head, *H'* = 300 m. In equations 6.28 and 6.29 Q_v and *H'* are in gpm and ft head, respectively. For the separator it was considered a vertical vessel of stainless steel 316, cost factor of 2.1. The separator cost depends on the weight, *W*, height, *L*, and internal diameter of the vessel, *D*, but these variables were assumed to be constant. They values considered were of *W* = 2000 lb, *L* = 2 m and *D* = 1 m and the units used in the correlations were lb, ft and ft, respectively.

$$\text{Cooler cost (\$)} = \frac{0.29(\frac{Q}{\Delta T})}{1.6} \tag{6.33}$$

Equation 6.33 was used to estimate the coolers cost assuming a constant (Q/ΔT) factor of 30 kW/K and the rest of the parameters were selected for treated cooling water and medium gas pressure [32].

Unlike all the rest of the economic section of the flowsheet that was taken from the reference case[26], the cost estimation for the main cryogenic heat exchanger was performed in the MSHX model developed in this work, as explained in chapter 5.1.

The cost correlations taken from [31] are related to the year of 2008 and the correlations from [32] are from 1994. This prices were updated to the year of 2014 with the CEPCI index, see table 6.4 and equation 6.34.

Table 6.4: CEPCI indexes.

Year	**CEPCI**
1994	368.1
2008	575.4
2014	575.7

$$\text{Updated price at year } \textit{new} = \text{Price at year } \textit{old} \times \frac{CEPCI_{new}}{CEPCI_{old}} \tag{6.34}$$

It is to be emphasised that the data and calculation procedures regarding this entire economics chapter was taken from [26] which economic analysis was done based on [30, 31, 32], with the exception of the main cryogenic exchanger cost presented in section 5.1. To allow for a fair comparison of the optimisation cases with the different exchanger models it was necessary to simulate the processes as similar as possible to state with certainty that the differences in optimisation time were related to this unit only.

This chapter shows that the NPV depends essentially on the LNG production (sales), the NG cost, and the utilities that depend essentially on the compressor power and the equipments cost.

6.3 Problem formulation

Optimisation is present in various levels of typical industry companies, from management to design to operation. The purpose of any optimisation is to find the values of the variables corresponding to the best possible value of a given objective function. An optimisation problem function can be linear or non-linear, and may be confined by various constraints. A general optimisation problem can be defined as follows:

$$\begin{aligned} \text{Minimise or maximise :} \quad & J = f(x) \\ \text{Subject to :} \quad & g(x) \leq 0 \\ & h(x) = 0\,. \end{aligned} \tag{6.35}$$

In equation 6.35, *J* represents the objective function, which is a function of variable(s) *x*. The optimisation problem may be subject to inequality *g(x)* and equality *h(x)* constraints.

Different optimisation methods have been developed in order to solve problems such as above. In the case where both objective function and constraints are linear functions of the variables, the optimisation becomes a linear programming problem. If either objective function or constraints are non-linear functions of the variables, the problem is non-linear and more sophisticated methods are required to solve it. In the present case gPROMS uses the solver NLPSQP to solve the problem as it assumes a non-linear behaviour. This solver employs a sequential quadratic programming (SQP) method for the solution of a non-linear programming problem (NLP). SQP is one of the most effective methods for non-linearly constrained optimisation problems. The method generates steps by solving quadratic sub-problems; it can be used both in line search and trust-region frameworks. The SQP method can be viewed as a generalization of Newton's method for unconstrained optimization in that it finds a step away from the current point by minimizing a quadratic model of the problem.

In this case the objective function was the Net Profit Value (NPV) of the SMR process, equation 6.36.

$$Maximise\ J = NPV \tag{6.36}$$

To maximise the NPV several design variables were selected due to having dominant effects on the performance and efficiency of SMR processes: mixed refrigerant's flowrate, composition, suction pressure and condensation pressure [33, 34, 35]. In MR cycles the refrigerant evaporates and condenses over two different pressure levels. Increasing the difference between these pressure levels prevents temperature crossing in the main exchanger but at the expense of increasing shaft work. There are optimal pressure differences for LNG exchangers that minimise temperature and shaft work. Refrigerant composition is the most flexible and significant variable in the design of MR systems, see chapter 2.3.2. It is important in avoiding temperature crossing in the main exchanger and minimizing shaft work. The variables changed to maximise the NPV are the control variables and are stated with the respective boundaries in table 6.5 and represented in figure 6.3. It should be noted that the objective function, control variables and constraints are the same and have the same initial values than the reference case [26] (with some minor changes) for purposes of optimisation time comparison.

The initial guesses of the decision (or control) variables are the same used in the initial simulation,

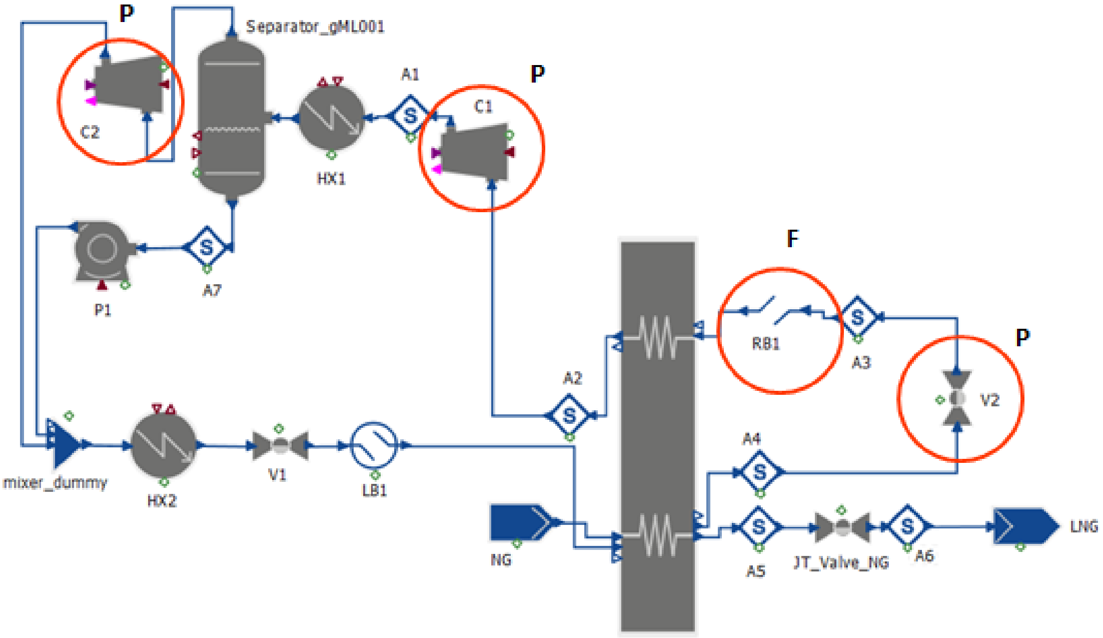

Figure 6.3: Representation of the control variables used in optimisation of the SMR process.

Table 6.5: Control variables, their bounds and initial guesses for optimisation.

Control variable	**Initial value**	**Lower bound**	**Upper bound**
Outlet pressure C1 (bar)	14	1	20
Outlet pressure C2 (bar)	52.37	10	60
Outlet pressure V2 (bar)	3.23	1	10
MR mass flowrate (kg/s)	4.669	1	15
MR components molar fraction			
Nitrogen	0.155	0	1
Methane	0.288	0	1
Ethane	0.345	0	1
Propane	0.022	0	1
Butane	0.19	0	1

section 6.3.1. This is important because running the initial simulation allows the verification of its feasibility and this will be the initialisation (initial iteration) of the optimisation. Besides the boundaries in control variables, the problem is also subject to some constraints presented in table 6.6.

Table 6.6: Constrained variables and their limits in the optimisation problem.

Constrained variable	**Lower bound**	**Upper bound**
Dew margin (K)	2	100
Compressor ratio C1	1.5	5
Compressor ratio C2	1.5	5
ΔT_{min} (K)	1.5	20

Dew margin is the difference between the MR cold stream outlet of the MCHX and the dew temperature of that stream at its pressure. This variable was constrained with a lower bound to prevent liquid formation in the suction part of the compressor. Regarding the compressor ratio boundaries, below 1.5 the compression is not significant to justify the use of a compressor and 5 was the value chosen for the maximum limit placed on compressors based on the maximum discharge temperature that is tolerable for the process and the mechanical equipment. A positive temperature difference between the two curves is required to avoid temperature crossing hence a decrease in efficiency as explained in chapter 5.3.1. The value of 1.5 may be seen either as a safety margin for the thermodynamic evaluations, or as a trade-off between the heat exchanger area and the operating cost.

6.3.1 Initialisation

The initial guesses of the control variables in table 6.5 are used in the initialisation of the optimisation problem. Before optimisation it is made an initial simulation with this values to verify the feasibility of the conditions or there is the risk of failing the optimisation in the first iteration. The initial values for both controls and rest of the operational variables are stated in tables 6.7 to 6.12. These were taken from [33], [34] and [35] and are the same used in the optimisation reference case [26] with some minor adaptations due to the differences in exchanger models. The results presented in this section are from the simulations executed in the present work.

Table 6.7: Natural gas initial conditions.

Natural gas inlet	
Pressure (bar)	60
Temperature (K)	298.15
Flowrate (kg/s)	1
Composition (mol/mol)	
Nitrogen	0.0037
Methane	0.9589
Ethane	0.0296
Propane	0.0072
Butane	0.0006

Table 6.8: Mixed refrigerant initial conditions.

Mixed refrigerant	
Flowrate (kg/s)	4.669
Composition (mol/mol)	
Nitrogen	0.1550
Methane	0.2880
Ethane	0.3450
Propane	0.0220
Butane	0.1900

Table 6.9: Compressors initial conditions.

Compressor	**C1**	**C2**
Isentropic efficientcy (%)	80	80
Mechanical efficientcy (%)	100	100
Outlet pressure (bar)	14	52.37

Table 6.10: Coolers initial conditions.

Cooler	**HX1**	**HX2**
Outlet temperature (K)	293.15	293.15
Pressure drop (bar)	0	0

The natural gas stream reaches the main cryogenic exchanger as critical fluid and Multiflash is not able to calculate the dew and bubble points, thus it is assigned 0 to the position that corresponds to the natural gas stream of the $cond$ and vol arrays mentioned in chapter 5.2.

The relevant results of the simulation obtained in the present work are presented in table 6.13. This simulation included 1429 variables and 1285 equations. The optimisation starts from a NPV of 4.20M$.

Table 6.11: Other process pressures in initial simulation.

Pressure (bar)	
Pump outlet pressure	52.37
V1 pressure drop	0.001
V2 outlet pressure	3.23
LNG valve outlet pressure	1.05

Table 6.12: Main cryogenic heat exchanger initial conditions.

MCHX	
LNG outlet temperature (K)	109.45013
Hot MR outlet temperature (K)	109.452446
All pressure drops (bar)	0
Number of intervals (all streams)	9

Table 6.13: Main results of the initial simulation.

Results	
Total compression power (kW)	1256
MR cold outlet temperature (K)	282.15
ΔT_{min} (K)	4.23
Electricity cost (k$)	704
MCHX cost (k$)	855
NPV (M$)	4.20

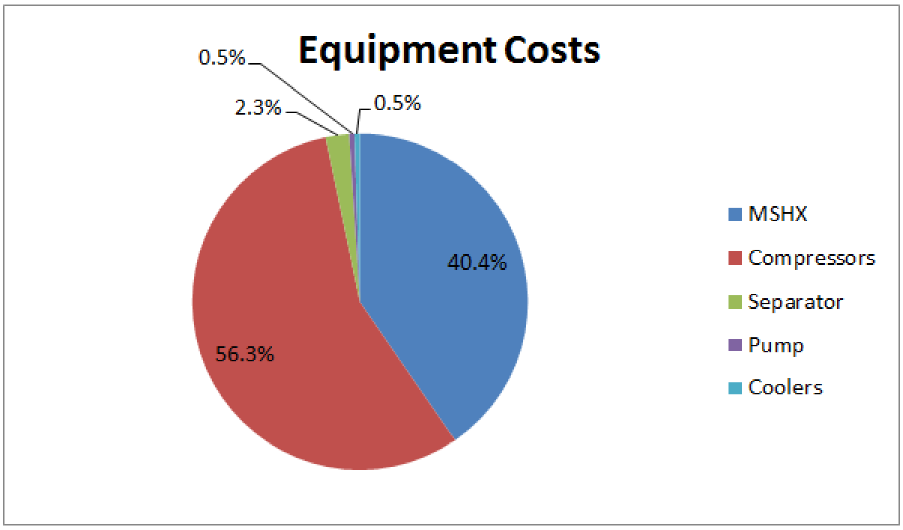

Figure 6.4: Distribution of the fraction of each main equipment cost on total equipment cost for the SMR process.

As can be observed in figure 6.4 the greater contribution for the total cost of equipments is the cost of compressors representing 56% followed by the cost of the cryogenic heat exchanger, 40%. This means that the compressors power and the factor $(Q/\Delta T_{ln})$ of the MSHX are very relevant for the NPV as the base of the economic calculations is the total cost of the purchased equipment. This figure also justifies the fact that the separator, pump and coolers costs were assumed to be constant, because they have no great impact in the total equipment cost and consequently in the NPV.

6.4 Optimisation results

The optimisation performed in the present work resulted in a NPV of 5.92M$. The optimum values of the decision variables and the constrained variables are stated in tables 6.14 and 6.15, respectively. In fact, the ”real” optimum values were not found because the optimisation run was terminated by lack of improvement both in optimisation variables and in objective function. This is represented in the execution output (report) as a stationarity criterion that should be lower than 0.001 and in this case it was 1.84. This means that, due to numerical issues the solver could not overcome, the optimisation did not reach the global optimum but achieved a better state than the initial as can be seen by the increase in NPV.

Table 6.14: Optimisation results of present work: decision variables.

Control variable	Optimum value	Lower bound	Upper bound
Outlet pressure C1 (bar)	6.455	1	20
Outlet pressure C2 (bar)	32.28	10	60
Outlet pressure V2 (bar)	1.29	1	10
MR mass flowrate (kg/s)	3.851	1	15
MR components molar fraction			
Nitrogen	0.051	0	1
Methane	0.305	0	1
Ethane	0.310	0	1
Propane	0.105	0	1
Butane	0.229	0	1

Table 6.15: Optimisation results of present work: constraints.

Constrained variable	Final value	Lower bound	Upper bound
Dew margin (K)	42.8	2	100
Compressor ratio C1	5	1.5	5
Compressor ratio C2	5	1.5	5
ΔT_{min} (K)	1.5	1.5	20

These values of control variables resulted in a MSHX cost of 0.76M$, electricity cost of 0.66M$ and 1.5K of minimum temperature approach. The optimisation increased the NPV in 41% by decreasing the energy requirements in 6% and the MSHX cost in 12%.

6.5 Optimisation comparison with reference case

As stated before, the optimisation performed in this work reproduced the optimisation problem of a reference case [26]. The comparison of the cases is described in this section.

6.5.1 Results

Table 6.16 presents the relative deviation of the relevant results of the initialisation of the present work compared with the one in the reference case [26]. The initialization is the first iteration of the optimisation, meaning it is the simulation of the initial guesses of the controls, data in section 6.3.1. The minimum temperature approach and the MCHX cost are of special importance because they are directly related to the exchanger model and NPV is the objective function of the optimisation. It can be observed that there is a high difference in the cost of the MCHX, and consequently in the NPV. As none of the works were validated with experimental data, it becomes very difficult to ascertain which one has a better cost estimation. This implies that the optimisation does not start from a similar point making the comparison of optimisation results, tables 6.17 and 6.18, also very difficult. It is important to mention that the optimisation performed in the reference case also ended due to lack of improvement, similarly to the optimisation in this work, which presents an additional difficulty in comparing the optimisation results.

Table 6.16: Initialisation results comparison.

Variable	**Relative difference (%)**
ΔT_{min}	0.1
MCHX cost	58.3
NPV	-121.0

As was expected, the global heat balance provides the same results in both cases as well as the calculations that do not involve the Pinch model, like the compressors power. The problem formulation of the reference case is very similar to the one described in chapter 6.3 with the heat transfer areas of NG and MR sides as additional decision variables.

Table 6.17: Optimisation results comparison: controls.

Variable	**Relative difference (%)**
Outlet pressure C1	-90.5
Outlet pressure C2	-24.2
Outlet pressure V2	-90.5
MR mass flowrate	-5.3
MR components molar fraction	
Nitrogen	-172.7
Methane	25.7
Ethane	-18.0
Propane	100.0
Butane	-17.1

Table 6.18: Optimisation results comparison: MCHX cost and NPV.

Variable	**Relative difference (%)**
MCHX cost	53.9
NPV	-104.7

It is very difficult to compare the results on a fair basis since right from the initial simulation with the same conditions the MSHX cost is different in 58%. This is mainly due to the different assumptions used in the MSHX models. Although both models use the C value method, the Pinch model calculates the cost of each interval that divides the heat transfer of the streams (composite curves) while the reference case model uses the total heat transferred determined in the heat balance and the global mean logarithmic temperature difference. In the reference case model the heat balances are calculated regarding the heat transfer areas given as input. This difference in the cost of the exchanger has a great influence in the objective function, NPV, that consequently also presents a high relative difference.

6.5.2 Optimisation time

In order to create a comparable environment for the optimisation cases it was necessary to rearrange the solution parameters of the processes so that the optimisations could run with similar number of iterations. Regarding an optimisation solver there are different types of iterations: major and minor. Major iterations evaluate the objective function (being maximised in this case) and calculate gradients of the objective function related to the control variables to decide in which direction to go, while minor iterations simply evaluate the objective function. As the first ones are more expensive to perform in terms of computational calculation, and consequently in simulation time, to do a fair comparison between optimisation times these need to have similar number of total iterations and the same proportion between major and minor iterations. As it can be observed in table 6.19 the number of iterations and line search steps is very different when comparing the two optimisation cases, which infers a different computational effort.

Table 6.19: Comparison of optimisation statistics.

Statistic parameter	**Pinch optimisation**	**Reference case [26]**
Number of iterations (major)	94	414
Number of line search steps (minor iterations)	330	833
No. of equations	1806	1284
Optimisation time (s)	240	560

The optimisation time of the reference case does not appear to be significantly big to justify a whole project to build a simple tool to decrease it. But this was a single case optimisation, for multi model optimisation like other cases performed in [26], it spent more than 1h, sometimes around 5h. And if the pressure drop mode of the MSHX was turned on in the reference case, the optimisation time would be even longer. The model developed here was to proof the concept of the possibility of a reduction in optimisation time of this kind of process.

To approximate the number of minor and major iterations in optimisation, the maximum line search step length was reduced from 1 to 0.01 which made the optimisations much slower as an iteration could not perform a greater step in the search for the optimum. To have the same number of iterations in both cases the maximum number of functions was reduced from 10000 to 50. Therefore the simulations did not achieve the optimum and failed prematurely but the time between optimisation cases became comparable. The statistics of this comparison are stated in table 6.20.

The optimisation with the Pinch model reduced the time in 60% compared to the reference case. Table 6.21 contains the fraction of optimisation time spent by the Foreign Objects used by the MSHX Pinch model. This evaluation of time distribution during optimisation with the Pinch model allows the better understanding of the model calculations and concedes the possibility of focus on bottlenecks for future changes to make the model even more efficient. It is to be noticed that the time used during

Table 6.20: Comparison of optimisation statistics with 49 iterations.

Statistic parameter	Pinch optimisation	Reference case [26]
Number of iterations (major)	49	49
Number of line search steps (minor iterations)	49	49
Total CPU time (s)	28.7	72.0

optimisation in Pinch FO calls represents only 0.5% of the total time while PHflash calls take 30% of the time which means a significant amount of total time is spent building the temperature grid in the Grid model.

Table 6.21: Foreign objects statistics in optimisation with Pinch model.

Statistic parameter	PHflash	Pinch
No. of calls	10130	5
No. of calls for derivatives	3020	200
Time of calls (s)	7.36	0.02
Time of calls for derivatives (s)	1.15	0.14
Fraction of time spent in calls (%)	30	0.5

The objective of building a model for a MSHX that would allow for simpler and consequently faster optimisations was achieved and though the comparison of results was not fair, the model built in the present work presents potential to be used in fast optimisations of cryogenic processes.

Chapter 7

Conclusions and future work

To summarise the work, a model for a MSHX was built in gPROMS and C++ with a simple tool to estimate the area and/or the cost of the exchanger based on the Pinch Analysis. The model provides the drawing of the composite curves and predicts minimal approach temperature. This model was integrated in a SMR flowsheet that was then optimised for purposes of optimisation time comparison with a reference case with a different MCHX model.

7.1 Conclusions

In the present work a mathematical model was built to simulate a multi-stream heat exchanger, unit used in cryogenic applications. The model is composed of 3 parts, 2 gPROMS models to calculate mass and heat balances, build grids and determine streams' properties; and a Foreign Object written in C++ language as an adaptation of the Pinch Analysis for MSHXs. The Pinch FO contains 2 methods, the one used in optimisation is applied to MSHXs and the other regards utility consumption being better used for networks of simple heat exchangers. The model is working as expected which was confirmed by a comparison of results against a software of heat integration, named Hint, with the same data as inputs.

The main idea of the project was to develop a model for a generic MSHX that was not adapted to any particular geometry and with a tool to calculate the cost and/or the area. With this tool the developed model can be used in cryogenic processes as the main cryogenic heat exchanger. In this work the process chosen was the PRICO with a SMR cycle with an incorporated cost model. The use of an exchanger with a cost option provided the possibility of optimisation of the process with economic objective functions.

The SMR gPROMS flowsheet was taken from a reference case [26] and the cryogenic exchanger was replaced with the model built in this project. The results of the initial simulations were very different in terms of cryogenic exchanger cost, and consequently profit objective function. This makes the comparison of the optimisation results with the reference case much difficult because the optimisations did not start from the same initial point. The different prediction of area/cost is essentially due to the different assumptions used in the exchanger models. Besides, both optimisation run cases ended due to lack of improvement which means the global optimum was not found. Even so, the objective function NPV improved 41% with the optimisation done in this work.

Despite the difficulty in comparison of results, a comparison of optimisation time was performed. The optimisation case implemented in the present work resulted in an optimisation time reduction of 60% for 98 iterations. This means that although the comparison of results is not fair, it is reasonable to state that the model built in this work has great potential for less time consuming optimisations. The distribution of the optimisation time in the present work was evaluated and the results demonstrated that the Pinch FO used only 0.5% of the total optimisation time, while PHFlash took 30%, both results including derivatives calculation times.

7.2 Future work

To build models with good predictions and small computation time to use in cryogenic processes simulations and optimisations is very important because it permits a better understanding of the process behaviour and saves time and money by providing the fewer configuration of the experimental work. For this and because this is a research area with much potential, this section presents some future work suggestions.

To start, the Pinch model should be validated to verify the accuracy of the cost calculation. Then both Pinch model and reference case model should be simplified so that the optimisations can start from a similar point making their optimisation results and times more fairly comparable.

The second method of the Pinch FO that regards utility consumption can be used for calculation of the area and cost of a whole network of two-stream heat exchangers. A suggestion for the future is to complete the algorithm in order to provide the design of the network of exchangers by defining matches between process streams.

Finally, the possibility of analytical derivatives determination should be studied and, if possible, implement this calculation to decrease the computation effort of the Pinch FO.

Bibliography

[1] Saeid Mokhatab and John Y. Mak et al. *Handbook of Liquefied Natural Gas*. Elsevier, 1^{st} edition, 2014. ISBN–13: 978-0-12-404585-9.

[2] Leidos Inc. Global Natural Gas Markets Overview. Technical report, EIA, 2014.

[3] Anselmo Buso and Monica Giomo. Mathematical modeling in chemical engineering: A tool to analyse complex systems. Technical report, Department of Chemical Engineering, University of Padova, 2011.

[4] Saeid Mokhatab and William A. Poe et al. *Handbook of Natural Gas Transmission and Processing*. Elsevier, 2006. ISBN 13: 978–0–7506–7776–9.

[5] Georg Hammer and Torsten Lubcke et al. *Ullmann's Encyclopedia of Industrial Chemistry*. Wiley-VCH Verlag GmbH and Co. KGaA, 2012.

[6] Arthur J. Kidnay and William R. Parrish. *Fundamentals of Natural Gas Processing*. Taylor and Francis, 1^{st} edition, 2006.

[7] Ecology and environment inc. Natural Gas nature's choice for clean energy. `http://www.nationalfuelgas.com/natural_gas_environment.aspx`. Accessed April, 2015.

[8] World Energy Resources. Technical report, World Energy Counsil, 2013.

[9] World LNG Report. Technical report, International Gas Union, 2014.

[10] World LNG Report. Technical report, International Gas Union, 2015.

[11] LNG journal. `http://www.lngjournal.com/lng/`. Accessed April, 2015.

[12] Terrence F. Yee and Ignacio E. Grossmann et al. Simultaneous optimization models for heat integration. *Carnegie Mello University: Engineering Design Research Center*, 1990.

[13] M. M. Faruque Hasan and Iftekhar A. Karimi et al. Modelling and simulation of main cryogenic heat exchanger in a base-load liquefied natural gas plant. *17th European Symposium on Computer Aided Process Engineering*, 2007.

[14] R. S. Kamath and I. E. Grossman et al. Modelling multistream heat exchangers with and without phase changes for simultaneous optimization and heat integration. *Wiley Online Library*, 2011.

[15] The Chemical Engineers' Resource Page. Pinch technology: Basics for the beginners.

[16] Linnhoff March. Introduction to pinch technology, 1998.

[17] Robin Smith. *Chemical Process: Design and Integration*. John Wiley & Sons Ltd., 2005.

[18] D. L. Westphalen and M. R. Wolf Maciel. Pinch analysis based on rigorous physical properties. *Brazilian Journal of Chemical Engineering*, 16, September 1999.

[19] Process Systems Enterprise Limited. `http://www.psenterprise.com/`, May 2015.

[20] Process Systems Enterprise Limited. gproms ProcessBuilder documentation, July 2015. version 1.0.0.

[21] System programmer guide. Technical report, Process Systems Enterprise Limited, 2013. version 3.7.

[22] Foreign objects and foreign processes. Technical report, Process Systems Enterprise Limited, 2013. version 3.7.

[23] User guide for models and physical properties. Technical report, Infochem Computer Services Ltd, 2013. version 4.3.

[24] Geoff F. Hewitt and Simon J. Pugh. Approximate design and costing methods for heat exchangers. *Heat Transfer Engineering*, 2007.

[25] A. Salama and A. Khalil. Optimization of plate fin heat exchangers used in natural gas liquefaction. *Tenth International Congress of Fluid Dynamics*, 2010.

[26] Joungho Park. Refrigerant optimization for integrated design and control of cryogenic systems under uncertainty. Master's thesis, Imperial College London, 2015.

[27] Kuppan Thulukkanam. *Heat Exchanger Design Handbook*. CRC Press, 2^{nd} edition, 2013.

[28] Ángel Martín and Fidel A. Mato. Hint: An educational software for heat exchanger network design with the pinch method. *Department of Chemical Engineering and Environmental Technology, University of Valladolid, Spain*, 2007.

[29] Dionysis Zindros. A gentle introduction to algorithm complexity analysis. `http://discrete.gr/complexity/`. Accessed August, 2015.

[30] Klaus D. Timmerhaus Max S. Peters. *Plant Design and Economics for Chemical Engineers*. McGraw-Hill, 2^{nd} edition, 2014.

[31] James R. Couper and Stanley M. Walas et al. *Chemical Process Equipment Selection and Design*. Elsevier, 3^{rd} edition, 2012.

[32] Geoffrey Hewitt and G. L. Shires et al. *Process Heat Transfer*. CRC Press, 1^{st} edition, 1994.

[33] A. Aspelund and T. Gundersen et al. An optimization-simulation model for a simple LNG process. *Elsevier: Computers and Chemical Engineering*, 2009.

[34] M. Mokarizadeh Haghighi Shirazi and D. Mowla. Energy optimization for liquefaction process of natural gas in peak shaving plant. *Elsevier: Energy*, 2010.

[35] Per Eilif Wahl and Sigurd Weidemann Lovseth et al. Optimization of a simple LNG process using sequential quadratic programming. *Elsevier: Computers and Chemical Engineering*, 2013.